HHS Public Access

Author manuscript

Inorg Chem. Author manuscript; available in PMC 2018 December 05.

Published in final edited form as:

Inorg Chem. 2018 March 05; 57(5): 2333–2350. doi:10.1021/acs.inorgchem.7b02912.

Synthesis and Applications of Perfunctionalized Boron Clusters

Jonathan C. Axtell[†,*], **Liban M. A. Saleh**[†], **Elaine A. Qian**[†,‡,§], **Alex I. Wixtrom**[†], and **Alexander M. Spokoyny**[†,§,*]

[†]Department of Chemistry and Biochemistry, University of California, Los Angeles, 607 Charles E. Young Drive East, Los Angeles, CA 90095, United States

[‡]Department of Bioengineering, University of California, Los Angeles, 420 Westwood Plaza, Los Angeles, CA 90095, United States

[§]California NanoSystems Institute (CNSI), University of California, Los Angeles, 570 Westwood Plaza, Los Angeles, CA 90095, United States

Abstract

This Viewpoint Article describes major advances pertaining to perfunctionalized boron clusters in synthesis and their respective applications. The first portion of this work highlights key synthetic methods allowing one to access a wide range of polyhedral boranes (B_4 and $B_6 – B_{12}$ cluster cores) that contain exhaustively functionalized vertices. The second portion of this Viewpoint showcases the historical developments in using these molecules for applications ranging from materials science to medicine. Lastly, we suggest potential new directions for these clusters as they apply to both synthetic methods and applications.

Graphical abstract

The present Viewpoint Article summarizes the syntheses and applications of perfunctionalized boron clusters with particular highlights on foundational works as well as the most up-to-date examples. We also provide a brief outlook on the field as it stands in the context of potential further development and application of boron cluster chemistry to solve pressing problems in chemistry, materials science and medicine.

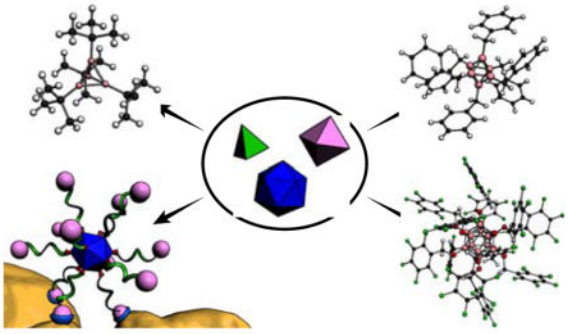

[*]Corresponding Author: spokoyny@chem.ucla.edu, axtell@chem.ucla.edu.

Author Contributions

The manuscript was written through contributions of all authors. All authors have given approval to the final version of the manuscript.

Introduction

Carbon-based chemistry has been at the forefront of chemical research and has occupied the thoughts and efforts of its leading exponents for over two centuries. Despite its proximity to carbon in the periodic table, boron-based chemistry (though rich) has lagged far behind its first-row neighbor and in most cases has been used in service of carbon-based chemistry,[1] rather than as a building block in its own right.

For boron chemistry, the history of borane (or boron hydride) chemistry began with the pioneering work of Alfred Stock, who with his co-workers isolated a series of simple boranes, including the classic diborane(6) B_2H_6.[2] However, it was not until the theoretical prediction of the icosahedral borane $[B_{12}H_{12}]$ by Lipscomb and co-workers in 1954 that the unusual nature of the bonding in boranes become apparent. Here, the concept of boron clusters was introduced,[3] with subsequent studies by Longuet-Higgins and Roberts suggesting that the stable form of this icosahedron would have an overall 2- charge.[4] These theoretical studies were then validated by Hawthorne and Pitochelli in a series of reports highlighting the first synthesis of dodecaborate $[B_{12}H_{12}]^{2-}$ as well as decaborate $[B_{10}H_{10}]^{2-}$ species.[5,6]

Contemporary books and reviews have broadly showcased recent advances in boron cluster chemistry and their applications,[7–19] but in this Viewpoint we hope to reveal to the wider inorganic chemistry community the immense potential of boron clusters by focusing on a particular class of molecules, namely perfunctionalized clusters whose cores are composed entirely of boron atoms. We will discuss their synthesis and unique attributes and then present examples of their use in some unusual and unexpected arenas, ranging from photo-activation of olefins to hybrid nanomolecules. Finally, we will discuss potential future directions for these unique molecules and hope to provide inspiration for the wider community to engage in boron cluster chemistry.

Definition of a Cluster in this Viewpoint

In this Viewpoint, we will be discussing the synthesis and applications of perfunctionalized all-boron clusters. Here the clusters are in their *closo* polyhedral forms as defined by Wade,[20] where *n* number of boron atoms contain (*n*+1) skeletal bonding electron pairs, typically resulting in anions of the type *closo*-$[B_xH_x]^{2-}$ (x = 6 – 12 and above). These molecules exhibit unique bonding situations characterized by multicenter, two electron bonding and three-dimensional aromaticity and electron delocalization. These characteristics are believed to contribute to the high stability of these species and have been reviewed in the literature.[21] This bonding situation is qualitatively visualized in 1) one set of atomic orbitals whose radial extension toward the center of the cluster results in the in-phase overlap of *n* boron-based orbitals of a cluster of the general formula $B_xH_x^{y-}$, forming a molecular orbital in the center of the cluster shared by all boron atoms and 2) one set of atomic orbitals whose in-phase contributions result in a molecular orbital delocalized over the surface of the pseudo-spherical cage (Fig. 1A–B). For thoroughness, some perfunctionalized boron cluster classes will be addressed that deviate from Wade's rules, such as the 4-membered polyhedral boron clusters and charge-neutral boron subhalides that have been reported. Furthermore, in

addition to the expected *closo*-$[B_xH_x]^{2-}$ boron cluster forms (x = 6 – 12), we will show that perfunctionalization of such molecules can also lead to *hypocloso*-$[B_xH_x]^{1-}$ and *hypercloso*-$[B_xH_x]^0$ derivatives. Insofar as the parentage of these monoanionic and neutral species lie in boron clusters that abide by Wade's rules, they will be included in this Viewpoint.

Synthesis of Perfunctionalized Boron Clusters

B_4 and B_6 Clusters

The smallest boron-based clusters known are the deltahedral tetraboranes.[22,23] In contrast to higher-membered congeners (e.g., B_6 or B_{12}), these clusters do not display the expected $2n$ +2 bonding electron count that is commonly encountered in 3D-aromatic boron clusters.[21,24] The first known boron tetrahedrane, tetraboron tetrachloride,[25] was reported in 1952 as a thermal decomposition product of B_2Cl_4 (Fig. 2), obtained only in small yields; its solid-state X-ray structure was subsequently solved in 1953.[26] The early procedures for synthesizing this molecule involved either electrical or microwave discharges in the presence of BCl_3 and mercury,[23] with more recent procedures that produce workable yields involving the reduction of R–BF_2 fragments by Na/K alloy in alkane solvents.[27,28] Alternatively, $B_4R_nCl_{4-n}$ (n = 1, 2, 4) analogues have been synthesized through treatment of the halogenated B_4Cl_4 cluster with alkyllithium reagents.[29,30] The reactivity of B_4Cl_4 has been described by Morrison and is summarized in Fig. 2.[30]

From haloaminoborane precursors, Siebert and co-workers synthesized tetraborane compounds of the type $B_4(NR_2)_4$ (R = Me, Et, ^{i}Pr, or NR_2 = 2,2,6,6-tetramethylpiperidinyl (TMP)).[31] However only in the cases of R = Et or TMP were *closo*-tetraborane products obtained; the other derivatives were isolated as cage-opened species. Mention has also been made of a tetramesityltetraborane, though to our knowledge this molecule has not been published.[32] Finally, Paetzold and co-workers have reported the synthesis of neopentyl and mixed alkyl tetraborate derivatives, however these neutral compounds were obtained in yields of 5% or less.[33]

In comparison to larger cluster congeners, the functionalization and applications of 6-membered, *closo*-$[B_6H_6]^{2-}$ clusters is largely underdeveloped. Most of chemistry conducted with these species was performed by Preetz and co-workers, who showed that in contrast to the typical Lewis acidity and high electrophilicity of tricoordinate boron, the hexaborate dianion is in fact *nucleophilic* at boron. It is generally accepted that this nucleophilicity is a result of the maxima of electron-density residing at each face of the hexaborate octahedron. A Microreview by Preetz and Peters describes the majority of the synthesis and substitution chemistry of *closo*-$[B_6H_6]^{2-}$ clusters.[34] It is noteworthy, however, that the issue of hexaborate peralkylation was addressed briefly in this account, in which it was suggested that only up to three vertex substitutions by alkyl substituents were possible as a consequence of the steric crowding of alkyl substituents and difficulty in facial proton removal prior to further substitution (*vide supra*). We have recently discovered, however, that under appropriate conditions, perfunctionalization is in fact possible (*vide infra*).

The first mention of a perfunctionalized *closo*-$[B_6H_6]^{2-}$ species was made by Klandberg and Muetterties in 1966.[35] However, not until almost 20 years later was a directed preparation of

perhalogenated hexaborate dianions disclosed by Preetz and Fritze *via* treatment of $Na_2[B_6H_6]$ with halogen in basic, aqueous media to produce *closo*-$[B_6X_6]^{2-}$ (X = Cl, Br or I).[36] The resulting compounds were thoroughly studied by IR and Raman spectroscopy,[37] as well as ^{11}B NMR spectroscopy, which revealed an upfield shift of boron resonances from *closo*-$[B_6Cl_6]^{2-}$ to *closo*-$[B_6Br_6]^{2-}$ to *closo*-$[B_6I_6]^{2-}$.[38] Subsequently, it was discovered that halogenation could be performed using succinimide-based reagents, however these conditions were employed largely for synthesizing only partially halogenated derivatives (Fig. 3).[39]

In cases of either diatomic halogen or NXS-based halogenation, species of the type *closo*-$[B_6X_nH_{6-n}]^{2-}$ (n = 1 – 5) were generally observed, opening the possibility for heteroleptic perhalogenated *closo*-hexaborates. Interestingly, the synthesis of the disclosed *bis*-heteroleptic perhalogenated hexaborates, which form under analogous conditions to homoleptic perhalogenated derivatives, require a specific, sequential treatment with halogen, in which the more electronegative halogen must first be charged to the hexaborate cluster, followed by the less electronegative halogen.[39,40] In this way, halogenated hexaborate clusters of the types *closo*-$[B_6Cl_nBr_{6-n}]^{2-}$, *closo*-$[B_6Cl_nI_{6-n}]^{2-}$, and *closo*-$[B_6Br_nI_{6-n}]^{2-}$ may be synthesized. To the best of our knowledge, the chemistry of these *bis*-heteroleptic clusters has not been further explored.

Prior to our involvement, the only non-halogen containing perfunctionalized six-membered *closo*-boron clusters were the neutral *hypercloso*-$B_6(NEt_2)_6$,[41,42] with Berndt and co-workers also disclosing the synthesis and structure of the dimethyl analogue, *hypercloso*-$B_6(NMe_2)_6$.[43] Given our interest in the development of chemistry and applications of perfunctionalized boron clusters,[44–46] we reexamined the reactivity of the *closo*-$[B_6H_7]^{1-}$ anion. Under microwave heating conditions, the hexaborate anion can be substituted with benzyl bromide electrophiles (Fig. 4A), affording a perfunctionalized cluster of the type *closo*-$[B_6(CH_2Ar)_6H^{fac}]^{1-}$ (Ar = C_6H_5, 4-Br-C_6H_4), containing six newly formed B–C bonds. Importantly, these cluster molecules can be isolated as moisture and air-stable solids. Crystallographic characterization of one derivative confirmed the formation of six B–C linkages. Interestingly, in contrast to the perhalogenated hexaborates reported by Preetz (*vide supra*), these alkylated clusters are marked by their relative oxidative instability, distinguishing them from the known redox-reversible substituted dodecaborate clusters (*vide infra*). Overall, it is clear that the original observations by Preetz suggesting that *closo*-$[B_6H_6]^{2-}$ cluster features nucleophilic reactivity at boron sites can be extended towards building complex perfunctionalized cluster scaffolds.

B_7–B_{11} Clusters

Moving beyond the small octahedral B_6 cluster, several additional three-dimensional $B_nH_n^{2-}$ clusters (n = 7 – 11) have been studied,[6,47,48] though with the exception of B_{10} decaborate clusters, there has been relatively little exploration of their functionalization. The perfunctionalization chemistry of *closo*-$[B_{10}H_{10}]^{2-}$ was developed somewhat in parallel to that of the *closo*-$[B_{12}H_{12}]^{2-}$ dodecaborate cluster in the early 1960s,[49–53] with several routes to diverse functionalized derivatives resulting in partial substitutions of the cage-bound hydrogens.[54] Despite this early progress, in the subsequent decades only halogenation

resulted in successful substitution of all B–H vertices to achieve perfunctionalization of the $B_nH_n^{2-}$ (n = 7 – 11) clusters to form species of the type $B_nX_n^{2-}$ (X = Cl, Br and I).[30,53,55–59]

In 1964, the first fully halogenated cluster in this series was the decaborate dianion, with $[B_{10}Cl_{10}]^{2-}$, $[B_{10}Br_{10}]^{2-}$, and $[B_{10}I_{10}]^{2-}$ all synthesized by treating $[B_{10}H_{10}]^{2-}$ with chlorine, bromine, and iodine, respectively.[53] Several other perhalogenated clusters were synthesized *via* the thermal decomposition of diboron tetrahalide B_2X_4 or boron trihalide BX_3, thus forming the perhalogenated clusters directly from these non-polyhedral precursors[55] rather than subjecting the boron hydride B_nH_n clusters to halogens directly. There is some mass spectral evidence suggesting that $B_9(t\text{-Bu})_9$ was formed from the reaction of $[B_8Cl_8]^{2-}$ with *tert*-butyl lithium,[60] but the supposed product was neither isolated nor fully characterized.

A more exhaustive history of the functionalization chemistry possible with these clusters that fall short of full persubstitution can be found in excellent reviews by Morrison[30] (for $B_{7–9,11}$) and Sivaev[54] (for B_{10}). The limited perfunctionalization observed over the past few decades can be largely attributed to lower stability of these clusters compared to *closo*-$[B_{12}H_{12}]^{2-}$, which precludes harsher functionalization strategies. The stability of the boron subhalide clusters was predicted from their valence state index to be 9>11>8>10≈7,[56] though experimental thermal stability of the neutral clusters B_nX_n was found to be 9>10>8≈7,[55] showing poor agreement between the two methods but confirming the significantly lower stability of these clusters compared to $[B_{12}H_{12}]^{2-}$. More recent investigations of these clusters have resulted in the X-ray crystallographic analysis of the structures as well as further functionalization, however the halogenated derivatives remain the only perfunctionalized clusters in the B_nH_n (n = 7–11) series to date.[57,61–64]

B_{12} Clusters

Due to its stability and commercial availability, the vast majority of reports on perfunctionalized boron clusters concern the deltahedral *closo*-dodecaborate dianion, *closo*-$[B_{12}H_{12}]^{2-}$. For clarity, the following sections will be partitioned into those concerning homoperfunctionalized (Fig. 5) and heteroperfunctionalized (Fig. 6) B_{12}-based clusters.

Homoperfunctionalized B_{12} Clusters

Halogenation—The first reported perfunctionalization of *closo*-$[B_{12}H_{12}]^{2-}$ involved direct perhalogenation with elemental chlorine, bromine and iodine, resulting in molecules of the type *closo*-$[B_{12}X_{12}]^{2-}$ (X = Cl, Br or I) that could be handled without decomposition under ambient conditions.[53] To avoid the use of chlorine gas, Ozerov and co-workers recently showed that perchlorination of *closo*-$[B_{12}H_{12}]^{2-}$ may be achieved using SO_2Cl_2 as a chlorinating agent, leading to a more operationally simple synthesis.[65] Perfluorination of *closo*-$[B_{12}H_{12}]^{2-}$ proved more difficult and was first achieved by Solntsev and co-workers in the early 1990's through the action of supercritical HF at 550°C, producing $Cs_2[B_{12}F_{12}]$ in 38 % yield.[66] Later, work by Strauss and co-workers described improved yields of *closo*-$[B_{12}F_{12}]^{2-}$ salts up to 74 % and could be carried out on multigram scale using non-specialized glassware.[67,68]

Hydroxylation—Hawthorne and co-workers reported the first successful perhydroxylation of dodecaborate by refluxing $Cs_2[B_{12}H_{12}]$ in 30 % H_2O_2 for several days to form $Cs_2[B_{12}(OH)_{12}]$.[69] Through cation exchange protocols, the $B_{12}(OH)_{12}^{2-}$ dianion can be isolated as a variety of metal, acid, or organic salts $M_2[B_{12}(OH)_{12}]$ (where M = Li^+, Na^+, K^+, Rb^+, Cs^+, $[H_3O]^+$, $[NH_4]^+$, $[N^nBu_4]^+$, $[(PPh_3)_2N]^+$).[70,71] Unlike their organic analogues, most perhydroxylated dodecaborate salts show low solubility in water, with only $Cs_2[B_{12}(OH)_{12}]$ showing appreciable solubility and $[N^nBu_4]_2[B_{12}(OH)_{12}]$ showing excellent solubility at slightly elevated temperatures. In addition, the tetra-*n*-butyl ammonium salt is soluble in organic solvents, making it a valuable precursor for further derivatization.

Esterification—$[N^nBu_4]_2[B_{12}(OH)_{12}]$ can be transformed into esters of the type $[N^nBu_4]_2[B_{12}(OC(O)R)_{12}]$ (R = Me or Ph) using acetic anhydride or benzoyl chloride, as reported by Hawthorne and co-workers. Later reports from the same laboratory further expanded the scope of substituents that could be installed on the $B_{12}(OH)_{12}^{2-}$ core through ester linkages.[72–74]

Etherification—*closo*-$[B_{12}(OH)_{12}]^{2-}$ reacts with a variety of alkyl or benzyl halides in the presence of base to form per-etherated clusters. The first such compound reported involved the reaction of $[(PPh_3)_2N]_2[B_{12}(OH)_{12}]$ with benzyl chloride and $^iPr_2NEt$ in refluxing acetonitrile for several days to form (after workup) $Na[(PPh_3)_2N][B_{12}(OCH_2Ph)_{12}]$ in 48 % yield.[75] A variety of other peretherated clusters were also reported using similar conditions.[71] Although these methods were effective, the length of time required for the reactions reduced their utility. To address this issue, our laboratory has reported a rapid microwave-assisted method to prepare peretherated clusters.[44] This method drastically reduces the reaction time from an average of multiple days to minutes to hours. Etherification of the perhydroxylated clusters has a profound effect on the redox properties of B_{12}-clusters and is discussed separately in the text (*vide infra*).

Heteroperfunctionalized B_{12} clusters

B–X/B–N functionalization—While Muetterties and co-workers reported a variety of B_{12} clusters containing B–X and B–N bonds as early as 1965, none of the molecules described were perfunctionalized.[76] Strauss and co-workers were successful in perfluorinating *closo*-$[H_3NB_{12}H_{11}]^{1-}$ to form *closo*-$[H_3NB_{12}F_{11}]^{1-}$ *in situ*, which could then be isolated *via* precipitation as the ammonium salt $[N^nBu_4]_2[H_2NB_{12}F_{11}]$.[77] An important feature of *closo*-$[H_3NB_{12}F_{11}]^{1-}$ is the reduction of the overall charge on the cluster from 2- to 1- as a result of charge compensation by the ammonium fragment. In principle, this allows the cluster to be treated as an analogue of the significantly more expensive polyhedral carba-*closo*-dodecaborate *closo*-$[CB_{11}F_{11}]^{1-}$, an exceptional weakly coordinating anion. Further functionalization of *closo*-$[H_3NB_{12}F_{11}]^{1-}$ at nitrogen affords dodecaborate anions of the type *closo*-$[R_3NB_{12}F_{11}]^{1-}$ (R = Me and *n*-$C_{12}H_{25}$). Jenne and co-workers were successful in the synthesis of the perchlorinated derivative *closo*-$[H_3NB_{12}Cl_{11}]^{1-}$ using $SbCl_5$ as a chlorinating reagent,[78] with further substitution then carried out at nitrogen to produce *closo*-$[Me_3NB_{12}Cl_{11}]^{1-}$. Duttwyler and co-workers later reported a simplified synthesis whereby $SbCl_5$ was replaced with SO_2Cl_2.[79]

B–X/B–O functionalization—Muetterties and co-workers reported the first example of a mixed halogenated/hydroxylated B_{12} cluster, *closo*-$[B_{12}F_{11}OH]^{2-}$, as a byproduct of the attempted perfluorination of *closo*-$[B_{12}H_{12}]^{2-}$ with elemental fluorine in water.[53] Jenne and Kirsch reported the synthesis of the heteroperfunctionalized cluster *closo*-$[B_{12}X_{11}OH]^{2-}$ and subsequent alkoxylation to form a variety of compounds of the type *closo*-$[B_{12}X_{11}OR]^{2-}$ (where X = Cl or Br; R = *n*-C_3H_7, *n*-C_8H_{17} or *n*-$C_{12}H_{25}$).[83] As with the formation of *closo*-$[H_3NB_{12}Cl_{11}]^{1-}$, Duttwyler and co-workers described a simplified synthesis of *closo*-$[B_{12}Cl_{11}OH]^{2-}$ using SO_2Cl_2 instead of chlorine gas and showed additional reactivity at the hydroxyl group to produce *closo*-$[B_{12}Cl_{11}O(SO_2CF_3)]^{2-}$ and *closo*-$[B_{12}Cl_{11}OTs]^{2-}$ respectively.[82] A summary of these functionalization methods is shown in Figure 5.

B–N/B–O functionalization—Hawthorne and co-workers synthesized the mixed B–N/B–O functionalized cluster *closo*-$[B_{12}(OH)_{11}(NH_3)]^{1-}$ *via* amination of *closo*-$[B_{12}H_{12}]^{2-}$ to form *closo*-$[B_{12}H_{11}(NH_3)]^{1-}$ followed by hydroxylation to form *closo*-$[B_{12}(OH)_{11}(NO_2)]^{2-}$ and a final reduction step with Raney nickel to afford the desired *closo*-$[B_{12}(OH)_{11}(NH_3)]^{1-}$ species.[84] The authors report that nitro derivative *closo*-$[B_{12}(OH)_{11}(NO_2)]^{2-}$ may be used directly for further functionalization of the hydroxyl group, with subsequent reduction to yield products of the type *closo*-$[B_{12}(OR)_{11}(NH_3)]^{1-}$ (see Figure 6).

Redox Chemistry of Perfunctionalized Clusters

Upon perfunctionalization, boron clusters can access electronic states that do not conform to Wade's rules. This gives rise to molecules that potentially have access to three distinct oxidation states: *closo*-$[B_xR_x]^{2-}$, *hypocloso*-$[B_xR_x]^{1-}$ and *hypercloso*-$[B_xR_x]^{0}$. For hexaborate clusters, this redox chemistry is readily accessible for the homoleptic perhalogenated cluster derivatives *closo*-$[B_6X_6]^{2-}$ (X = Cl, Br or I). Use of choice oxidants sees their transformation to their highly colored open shell radical monoanions, *hypocloso*-$[B_6X_6]^{1-}$ (X = Cl, Br or I).[85,86] In comparison to the oxidation potential of the parent *closo*-$[B_6H_6]^{2-}$ (0.86V vs. Ag/AgCl/LiCl), *closo*-$[B_6Cl_6]^{2-}$ and *closo*-$[B_6Br_6]^{2-}$ are *more easily* oxidized, with oxidation potentials lying at 0.58V and 0.77V, respectively; in contrast, *closo*-$[B_6I_6]^{2-}$ demonstrates approximately the same oxidation potential as *closo*-$[B_6H_6]^{2-}$ at 0.88V. The perhalogenated derivatives B_9X_9 (X = Cl, Br, I) were found to have two highly reversible, well-separated one-electron steps between the dianionic and neutral states, with significantly lower oxidation potentials compared to the $B_{12}X_{12}$ species (−0.63 V to −0.74 V vs Fc/Fc^+ for the 2- to 1- oxidation step for B_9X_9 clusters, compared to 1.68 V to 2.27 V vs Fc/Fc^+ for the same redox event with $B_{12}X_{12}$).[87,88]

As mentioned, the vast majority of reports on perfunctionalized boron clusters concern the 12-vertex polyhedral *closo*-$[B_{12}H_{12}]^{2-}$. This particular class of molecule has a rich redox chemistry that has only recently been exploited. Without modification, boron hydride clusters such as *closo*-$[B_{12}H_{12}]^{2-}$ have very high redox potentials, which can result in irreversible cluster degradation or the formation of B–B linked dimers when subjected to controlled oxidiation.[89] However, perfunctionalization of the *closo*-$[B_{12}H_{12}]^{2-}$ scaffold to form halogenated or other derivatives engenders reversible redox behavior.[11] Early examples of this phenomenon include reports that the perhalogenated dodecaborates could undergo single electron oxidation, forming a stable *hypocloso*-$[B_{12}X_{12}]^{1-}$ radical.[90] Attempted

isolation of one such species, $[B_{12}Cl_{12}]^{1-}$, instead resulted in the isolation of neutral $B_{12}Cl_{12}$, evidencing the structural stability but potentially high reactivity of these radicals.[91] However, other dodecaborate radicals, such as salts of perhydroxylated *closo*-$[B_{12}(OH)_{12}]^{1-}$ [92] as well as permethylated $[B_{12}Me_{12}]^{1-}$ [93] have been isolated as stable anions. Their stability is largely due to the 3-dimensional delocalization of electron density throughout the cluster core, which mitigates the potent reactivity of a localized radical (Fig. 7). Furthermore, steric protection of the cluster core through B-bound substituents also kinetically stabilizes the *hypocloso* species.

More recent explorations of this reversible redox behavior have been conducted with perfunctionalized derivatives of *closo*-$[B_{12}(OH)_{12}]^{2-}$. It was demonstrated that the ether-linked benzyl *closo*-$[B_{12}(OCH_2Ph)_{12}]^{2-}$ cluster can undergo two sequential, quasi-reversible one-electron oxidation reactions, enabling access to three distinct redox states: *closo*-$[B_{12}(OCH_2Ph)_{12}]^{2-}$, the stable radical *hypocloso*-$[B_{12}(OCH_2Ph)_{12}]^{1-}$, and the neutral *hypercloso*-$B_{12}(OCH_2Ph)_{12}$. In all three oxidation states, the dodecaborates were stable, isolable products that were fully structurally characterized.[75] The most useful feature of this redox behavior was the discovery that the individual redox potentials of the *closo*-$[B_{12}(OR)_{12}]^{2-}$ clusters could be rationally tuned — in a manner reminiscent of metal-based inorganic complexes — as a function of the *O*-bound alkyl or benzyl substituent.[11,71,94] Recent work has demonstrated even higher oxidation potentials for some newer *closo*-$[B_{12}(OR)_{12}]^{2-}$ derivatives, continuing the correlation between the predicted effects of the substituents (Fig. 8) while expanding the tunable window for the same redox event to a full 1 V (−0.61 V vs Fc/Fc^+ for the 1-/0 redox couple oxidation when R = *n*-hexyl, rising to +0.68 V vs Fc/Fc^+ for the same redox event when R = (3,5-bis)trifluoromethylbenzyl).[44,94]

Applications in Catalysis and Materials Chemistry

While boron clusters may have existed as chemical curiosities over the last century, they became a topic of intense interest for scientists during the 1950s, who, at the height of the space race, were keen to apply them towards the development of ever more powerful energetic materials for rocket fuels. Since interest quelled in the use of boron clusters in that arena, applications for boron clusters have been few and far between. Having outlined the state-of-the-art with regards to the synthesis of perfunctionalized boron clusters and extolled the virtues of their signature features, in this section of the Viewpoint we will highlight select examples of areas in which perfunctionalized clusters may be exploited.

Photoredox Behavior

Perfunctionalized carba-*closo*-dodecaborates of the type *closo*-$M[CB_{11}X_{11}]$ have found exceptional utility in homogeneous catalysis due to their ability to act as inert, extremely weakly coordinating anions.[96,97] While dodecaborates composed entirely of boron, which bear a charge of 2-, may be reminiscent of these weakly coordinating carboranes, the ability to functionalize these molecules and the properties that manifest as a result present a powerful opportunity to move perfunctionalized boron clusters away from a spectator role and towards being an active participant in reaction chemistry. In particular, the unique ability to tune the redox window of dodecaborates through perfunctionalization *via* judicious choice

of functional group (*vide supra*) provides straightforward access to air- and moisture-stable molecules that have well-defined one-electron redox chemistry across a range of potentials. Such redox chemistry could then be exploited to mediate a plethora of transformations across a range of substrates, irrespective of substrate reactivity.

During the course of our studies on improving the synthesis of ether linked perfunctionalized clusters,[44] we observed that solutions of *hypercloso*-$B_{12}(OCH_2Ph)_{12}$ left to stand in ambient light in the presence of with 4-methoxystyrene led to the formation of viscous mixtures; in the dark, no such mixture was obtained. By utilizing blue LEDs as a light source under controlled conditions, we demonstrated that the perfunctionalized cluster *hypercloso*-$B_{12}(OCH_2Ph)_{12}$ can behave as a powerful photooxidant in the visible light-assisted polymerization of olefins.[46] The proposed mechanism involves the generation of a potent photooxidant by visible light promotion of an electron from a low lying occupied orbital localized largely on the aryl rings and oxygens to the cluster-based LUMO (Fig. 9A). Unlike metal-initiated polymerizations of olefins which generally require an open coordination site for monomer approach, these clusters are devoid of well-defined coordination sites. It was therefore hypothesized that favorable, non-covalent interactions of the monomer and the aryl ring(s) of the benzyl substituents on the cluster periphery facilitate electron transfer from monomer to the dodecaborate core (Fig. 9B). Time-dependent Density Functional Theory (TD-DFT) studies carried out on both *hypercloso*-$B_{12}(OCH_2Ph)_{12}$ and *hypercloso*-$B_{12}(OCH_2C_6F_5)_{12}$ suggest that this charge-transfer excitation pathway is favorable and leads to an excited state species with a redox potential sufficiently anodic for the one-electron oxidation of styrene. Importantly, the energy of this excitation calculated *in silico* corresponds to the energy provided by a photon of blue (~450nm) light, which is consistent with the ~450nm absorption band observed for the benzyloxy-substituted *hypercloso*-B_{12}-based species (Fig. 9C). In order to render more electronically deactivated olefins reactive toward the B_{12}-based photoinitiators, enhancing the photooxidizing power of the *hypercloso*-cluster was required. Since the redox potential of perfunctionalized clusters can be tuned by varying the substituents bound to the cluster, more electron-withdrawing C_6F_5 groups were installed to form *hypercloso*-$B_{12}(OCH_2C_6F_5)_{12}$. The photooxidizing power was sufficiently increased to enable the activation of a large variety of olefins, including isobutylene, a notoriously difficult monomer that typically requires metal-based activators or harsh conditions (Fig. 9D).[98] Most impressively, these reactions were observed to proceed with as little as 0.005 mol % initiator loadings.

Applications as Weakly Coordinating Ions

Catalysis—Ozerov and co-workers have leveraged the weakly coordinating nature of *closo*-$[B_{12}X_{12}]^{2-}$ dianions in the catalytic hydrodefluorination (HDF) of sp^3 C–F bonds in the presence of silylium cations generated *in-situ* from H–$SiEt_3$.[65] In dichlorobenzene solvent, >97% HDF of 4-fluorobenzotrifluoride occurred at room temperature in 1h; the more challenging substrate, perfluorotoluene, likewise underwent HDF in 1h at 80°C. In both cases, perfect selectivity was observed for sp^3 C–F bonds and arene C–F bonds remained intact. This method is a clear proof-of-concept that perfunctionalized dodecaborates can be successfully employed as weakly coordinating anions under catalytic conditions. Furthermore, this example shows that these dianions can behave as competent

substitutes for carba-*closo*-dodecaborate analogues ($CB_{11}H_{11}^{1-}$ and functionalized derivatives) which, despite their well-established utility, are more difficult to synthesize, more expensive to purchase, and generally more difficult to perfunctionalize.

More recently, Kirsch and co-workers successfully employed a perfunctionalized boron cluster under gold catalysis conditions to effect a variety of ene-yne cyclization reactions. Single crystal X-ray structural data was also obtained which revealed a dimeric active catalyst and the weakly coordinating nature of the dodecaborate counterion.[99] The kinetic stability of these perfuctionalized boron clusters is particularly relevant to (cationic) transition metal catalysis, since even the widely used BAr^F anion ($[B(C_6F_5)_4]^-$) has been shown to engage in aryl ring transfer in the presence of transition metal cations.[100,101,102]

Reagents—The weakly coordinating nature of these dianions prompted Knapp and co-workers to employ $[CH_3]_2[B_{12}Cl_{12}]$ as a methylating agent. Me^+–Cl interactions stabilize the methyl cation however the dodecaborate framework remains intact. This compound is capable of methylating SO_2 as well as benzene to form $[CH_3OSO]_2[B_{12}Cl_{12}]$ and $[CH_3C_6H_6]_2[B_{12}Cl_{12}]$, respectively.[103] The same group later disclosed the stabilization of $[Al(CH_3)_2]^+$ using this dodecaborate anion.[104] It should be noted that Wehmschulte and co-workers reported a similar complexes employing a perfunctionalized dodecaborate as a counterion, including $[Ag(CH_3CN)][B_{12}Cl_{11}(NMe_3)]$, $[CPh_3][B_{12}Cl_{11}(NMe_3)]$, and $[Et_2Al][B_{12}Cl_{11}(NMe_3)]$.[105]

Superacids—Superacids have been used for many years to probe extremes of chemical behavior and engage interesting reactivity. Among the strongest are those based on carba-*closo*-dodecaborates, which like their neutral carborane and dianionic dodecaborate analogues exhibit chemical stability toward acidic solutions as well as charge delocalization which is thought to enhance acidic properties. And while most attention has been given to CB_{11}-based superacids, comparatively fewer studies have examined the acidity of dianionic dodecaborate derivatives. Muetterties and co-workers noted the extreme acidity of $B_{12}Cl_{12}$ and $B_{12}Br_{12}$ in the mid-1960s in which the authors disclosed their superior acidity to sulfuric acid.[53] More recently, experimental[106,107] and theoretical[107,108] efforts have been made to further quantify the (potential) acidity of such derivatives. In particular, Reed and co-workers showed[106] that $B_{12}Cl_{12}$ and $B_{12}Br_{12}$ exhibit comparable acidity to carborane acids and are sufficiently acidic to protonate benzene, which even trifluoromethanesulfonic acid and fluorosulfonic acid cannot do. Furthermore, *both* protons from $H_2B_{12}X_{12}$ are capable of arene protonation, not simply the first. This is a fundamental limitation of carborane acids and suggests potential for applications where superacidic conditions are necessary.

Ionic Liquids

Ionic liquids are gaining increased attention due to their unique chemical properties and potential applications.[109] Polyhedral boron clusters stand as viable candidates for such an application due to their known chemical and electrochemical stability as well as their tunability (*vide supra*). While usually encountered as solids, recent work has shown that these species may be appropriately functionalized to give low-melting (< 100°C) ionic

liquids. Jenne and Kirsch reported that perfunctionalized clusters of the type $[C_6mim]_2[B_{12}X_{11}OR]$ ($[C_6mim]^+$ = 1-hexyl-3-imidazolium) displayed decomposition temperatures well beyond 300°C for five of six derivatives. One of these, $[C_6mim]_2[B_{12}Cl_{11}(O\text{-}^nPr)]$ gave a melting point under 100°C.[83] More recently, the same group showed improved melting properties of dodecaborate-based ionic liquids using $[B_{12}X_6H_5NR_2]^{2-}$ and $[B_{12}X_6H_5NR_3]^-$ anions.[110] These compounds show low (as low as 57°C) melting points and high (> 2V) electrochemical stability, showing promise not only as ionic liquids but also as electrolytes. Notably, $[C_6mim][B_{12}Cl_6H_5N(^nPr)_3]$ shows a liquid range of over 300°C between melting (65°C) and decomposition (371°C).

Materials with cationic conductivity

In early works on Li-ion batteries, several research groups evaluated anionic boron clusters including *closo*-$[B_{12}Cl_{12}]^{2-}$ and *closo*-$[B_{10}Cl_{10}]^{2-}$ as electrolyte components.[111] For example, primary liquid cathode Li/$SOCl_2$ cells, which utilized $Li_2[B_{10}Cl_{10}]$ and $Li_2[B_{12}Cl_{12}]$ salts were reported in 1979.[112] Later, these electrolytes were tested in Li/TiS_2 cells by Exxon.[113,114] More recently, fluorinated all boron nanoclusters $Li_2[B_{10}F_{10}]$ and $Li_2[B_{12}F_{12}]$ salts were developed at Air Products (commercial name – "Stabilife fluorinated electrolyte salts"). The electrolyte solvent/salt formulation can be tuned to obtain promising cell cycling performance, especially at elevated temperature (60°C).[115,116] The high electrochemical stability of these anions has been shown to provide overcharge protection for 4V Li-ion batteries, shown with MCMB/spinel cells. Perfunctionalized cluster anions containing protons as counterions have been investigated for their potential use in proton conductor membranes. Early efforts testing $H_2[B_{12}Cl_{12}]$ however proved unsatisfactory for this application given significant decomposition of this cluster observed at elevated temperatures in aqueous media resulted from B-Cl bond hydrolysis.[90] In 2004, Stasko and co-workers reported the solid-state proton conductivity study of *closo*-$H_2[B_{12}(OH)_{12}]$, the conjugate acid of the $B_{12}(OH)_{12}$ dianion (Fig. 10).[117] The title compound was generated by treating *closo*-$Cs_2[B_{12}(OH)_{12}]$ with concentrated HCl at 150°C for 3d at ~8.5 atm. As with other dodecaborate based anions, *closo*-$H_2[B_{12}(OH)_{12}]$ displayed excellent thermal stability (>400°C in air or N_2 atmosphere). A proton conductivity of $1.5 \times 10^{-5}\ \Omega^{-1}\ cm^{-1}$ was measured for $H_2[B_{12}(OH)_{12}]$, which is an order of magnitude higher than that of known solid-state proton conductor $CsHSO_4$. This conductivity was shown to increase with increasing temperature. Distinct changes in proton dynamics at varying temperatures were also observed by solid-state ^1H NMR, corroborating the proton mobility hypothesis.

Very recently, Strauss and co-workers disclosed detailed studies of the coordination of $Na_2[B_{12}X_{12}]$ (X = F, Cl) and their hydrated forms to Na^+ ions in the solid state.[118] Interestingly, they concluded that $B_{12}Cl_{12}^{2-}$ coordinates Na^+ less strongly than $B_{12}F_{12}^{2-}$ and ultimately suggest that both perfunctionalized dodecaborate derivatives, in their dehydrated forms, may be viable candidates for ion conductivity in energy storage applications.

Biological Applications

A number of boron cluster derivatives are attractive candidates for a broad range of biomedical applications due to their exceptional stability and biocompatibility, availability of ^{10}B nuclei (20% natural abundance), and tunability.[52,119–121] Over the past few decades, many biological applications of boron clusters have been explored, most notably in the areas of drug delivery and imaging for the diagnosis and treatment of cancer,[7,119] and only most recently in the area of probing protein-biomolecule interactions.[45]

Delivery of ^{10}B for BNCT

The most widely investigated research area within boron cluster-based drug delivery is undoubtedly boron neutron capture therapy (BNCT), a binary therapeutic strategy for the treatment of cancer (Fig. 11A). The concept of BNCT was first proposed in 1936 by Locher,[122] and has since captured the attention of many researchers due to its elegant design. As described by Hawthorne and others, the beauty of BNCT lies in the fact that both of its essential components, nonradioactive ^{10}B nuclei and low-energy thermal neutrons, are nontoxic by themselves, however together they initiate an energetic nuclear decomposition reaction that typically cannot extend past the diameter of a cell.[10,119,123] Based on this principle, BNCT was proposed as a safer alternative to many of the single-component radiation and chemotherapy approaches for the treatment of cancer. Many boron-containing compounds have been investigated for BNCT with generally unsuccessful results, with the exception of L-*p*-dihydroxyborylphenylalanine (BPA) (Fig. 11B), which is still being used in the clinical settings today.[119,124,125] Between 1959 and 1960, the discovery of polyhedral borane anions *closo*-$[B_{10}H_{10}]^{2-}$ and *closo*-$[B_{12}H_{12}]^{2-}$ [5,6,126] sparked renewed interest in BNCT given the exceptional stability of these species and their high boron content. The sodium salt of $[B_{10}H_{10}]^{2-}$ (Fig. 11B) was tested in animals, and while it showed promising results, it later failed in a clinical trial.[127,128] Two thiol-containing derivatives, $Na_2[B_{10}Cl_8(SH)_2]$ and $Na_2[B_{12}H_{11}SH]$ (BSH) (Fig. 11B), were identified as potential drug candidates from studies using mouse tumor models.[128,129] Although $Na_2[B_{10}Cl_8(SH)_2]$ proved too toxic in mice, BSH exhibited more favorable properties and has since been extensively used in the clinical trials.[96,121,130]

However, despite the relative success of BPA and BSH in the clinical trials, an important challenge remains to selectively deliver sufficiently large amounts of ^{10}B nuclei to the tumor tissue (approximately 20–35 μg/g tumor or 10^9 atoms/cell), which is critical to the success of BNCT.[10,131] Therefore, two general approaches have been taken to tackle this issue. The first strategy involves the incorporation of boron into biomolecules with tumor-targeting abilities such as peptides and proteins, nucleic acids, carbohydrates, and porphyrins,[132,133] while the second approach uses liposomes and nanoparticles to deliver ^{10}B atoms to tumor tissues.[133–137] In particular, many boron-encapsulated and boron-lipid liposomes have shown promising results in their ability to selectively deliver therapeutic quantities of ^{10}B atoms into tumor cells for effective BNCT.[138–146]

However, while the liposome-based approach has been successful, this system is inherently inefficient, as only around 5–10 % of the total mass arises from boron.[73,147] In an attempt to improve the efficiency, boron cluster-based nanoparticles have been proposed as alternative

BNCT agents. Toward this end, Hawthorne and colleagues synthesized ester-linked[73] and ether-linked[147] derivatives of the dodecaborate core with pendant *nido-o*-carboranyl substituents, which in total contain roughly 40% boron content by mass. The sodium salt of the ether-linked cluster (Fig. 12) was found to be water-soluble and was subsequently evaluated for its suitability as a BNCT agent in a series of toxicity and biodistribution studies in animals.[147] The results from these studies indicate that the compound is non-toxic to mice at a therapeutic dose and tumor-selective (the tumor-to-blood ratio is 9.4), however in this particular study its accumulation in tumor tissues (10.5 μg/g tumor) was half of the therapeutic amount necessary for BNCT. Nevertheless, this strategy of using cluster-based nanoparticles as BNCT agents is appealing due to its high boron content, modularity, and low toxicity.

Very recently, Kovalska, Gumienna-Kontecka, and co-workers reported a spectroscopic and calorimetric binding study of perhalogenated decaborate ($[B_{10}X_{10}]^{2-}$, X = Cl, Br, I) and dodecaborate ($[B_{12}X_{12}]^{2-}$, X = Cl, I) dianions to bovine and human serum albumins (BSA and HSA, respectively) toward potential use in BNCT.[148] It was shown through isothermal titration calorimetry (ITC) and fluorescence quenching experiments that the halogenated boron clusters displayed a greater affinity toward albumin binding (~ 4–5 clusters per protein, $K \sim 10^4 - 10^6\ M^{-1}$) than the parent, $[B_nH_n]^{2-}$ (n = 10 or 12) cluster (2 clusters per protein, $K \sim 10^3\ M^{-1}$). Circular dichroism studies suggested that no significant change in the secondary protein structure had occurred even at the highest concentrations of cluster species tested, which is consistent with the inefficient fluorescence quenching of the HSA, which contains a Tyr residue buried within the protein manifold, relative to BSA, which contains both buried and surface Tyr residues, by all clusters examined. In a similar study, Losytskyy et al. studied the binding of oligoether- and ammonium-substituted decaborate anions to BSA, HSA, immunoglobin IgG, b-lactoglobulin, and lysozyme. It was found that the functionalized, charge-compensated B_{10}-based monoanions formed stronger interactions with these protein substrates than with unfunctionalized decaborate and dodecaborate dianions.[149] These studies present an additional delivery system for high boron content molecules *in vitro* and suggest that perhalogenated boron clusters may be potentially useful in BNCT applications.

Delivery of Chemotherapy Drugs

In addition to their function as BNCT agents, boron clusters have recently been developed as nanocarriers for the delivery of various chemotherapy drugs. Within the past few years, Hawthorne and colleagues have constructed several heterofunctional cluster-based drug delivery systems. For example, Bondarev *et al.* demonstrated the synthesis of a vertex-differentiated dodecaborate cluster scaffold, *closo*-$[B_{12}(OH)_{11}NH_3]^{1-}$, that is further functionalized with an amide-bound fluorescein and eleven carboplatin analogues bound through carbamate linkages.[84] This species is found to localize in the nuclei of A549 cancer cells and shows potent cytotoxicity against both platinum-sensitive and platinum-resistant cell lines.[84] In another example by Sarma *et al.*, a trimodal targeted drug delivery system was assembled from a hetero-perfunctionalized dodecaborate dianion, *closo*-$[B_{12}(OH)_{11}(OR)]^{2-}$, by conjugating one vertex to a fluorescein molecule *via* click chemistry and the eleven other vertices to a branched linker featuring both the targeting molecule glucosamine

and the anticancer drug chlorambucil (Fig. 13A).[150] Interestingly, the targeted cluster co-localized with the lysosomes (Fig. 13B) and mitochondria within Jurkat cancer cells and exhibited 15-fold enhanced cytotoxicity compared to the non-targeted cluster against cells overexpressing the receptor for glucosamine.[150] In a different approach to assembling the cluster-based nanocarriers, encapsulation of hydrophobic chemotherapy agent doxorubicin by the dendritic dodecaborate clusters in a manner reminiscent to its encapsulation by the poly(amidoamine) (PAMAM) dendrimers was disclosed,[151,152] thus laying the groundwork for potential delivery into cancer cells using funtionalized dodecaborates.

Diagnostic Imaging

In addition to their applications in drug delivery for various types of cancer treatments, many derivatives of boron clusters have also been investigated for potential applications in diagnostic imaging. In fact, for decades, radiolabeled boron clusters have been studied as X-ray contrast agents because the incorporation of radiolabels on boron clusters can lead to higher chemical stability of the radiolabels.[7] However, while there have been numerous reports on the radiolabeling of boron clusters,[7,13,153] the vast majority have focused on the radiolabeled carborane derivatives and therefore will not be discussed here.

We will instead examine the development of high-performance all-boron cluster-based contrast agents for a more modern imaging technique, magnetic resonance imaging (MRI). MRI has emerged as one of the most important tools for the diagnosis of diseases, however there is a need to develop larger MRI contrast agents that can overcome the issues of low relaxivity values, short plasma half-lives, and low contrast typically associated with low-molecular weight contrast agents, while remaining well-defined.[154–157] To tackle this challenge, Hawthorne and colleagues reported the synthesis of both the non-targeted[154] and targeted[157] (Fig. 14A) dodecaborate cluster-based MRI contrast agents that feature multiple gadolinium(III) complexes, and further demonstrated that these compounds provided significantly enhanced image contrast in addition to tumor-targeting ability provided by the cyclic RGD (cRGD) peptide (Fig. 14B).

Multivalent Protein Binders

We recently reported a strategy to rapidly assemble atomically precise, highly tunable organomimetic cluster nanomolecules (OCNs) *via* perfluoroaryl-thiol S_NAr chemistry (Fig. 15).[45] This approach is reminiscent of the facile assembly method of the thiol-capped gold nanoparticles (AuNPs), however the resulting OCNs are monodisperse and structurally robust under a range of biologically relevant conditions due to covalently-linked substituents on the cluster core.

Employing this strategy, the pentafluoroarylated dodecaborate clusters were perfunctionalized with a broad scope of thiolated (macro)molecules, including unprotected peptides, saccharides, and polymers. Furthermore, a glycosylated OCN was shown to be capable of *multivalent* interactions with Concanavalin A (Con A) (Fig. 16), resulting in binding affinities that are orders of magnitude higher than those observed for a single carbohydrate-lectin interaction. Taken together, this work showcases how one might rationally design and synthesize well-defined nanomolecules that can be useful in 1)

elucidating multivalent binding mechanisms and 2) potentially probing or inhibiting protein-biomolecule interactions.

Outlook and Conclusions

Beyond the applications mentioned above, perfunctionalized boron clusters remain relatively unexplored entities. Yet, these molecules represent a very unique class of building blocks for potential applications in materials science. For example, polymeric materials produced from boron-rich clusters have been disclosed as early as 1968,[158] but surprisingly, studies focused on producing functional, polymer-based materials featuring perfunctionalized boron cluster species have been extremely scarce. This is in contrast to a number of studies addressing the use of various carborane-based scaffolds for applications ranging from coatings to porous materials.[159,160] Thus, polymeric materials and surfaces featuring some of the halogenated clusters can expand the scope of existing materials and provide resins and supports featuring bulk “weakly coordinating” properties reminiscent of zeolites and other “weakly-coordinating” supports.[161] Similarly, polymers featuring anionic boron clusters as pendant functional groups should produce a unique class of polyelectrolytes. These materials can potentially show enhanced stabilities and tunable affinities toward cations, which in turn should allow one to tune ion mobility in the solid state providing access to materials with rationally tuned compositions and morphologies.[162] Furthermore, given the inherent three-dimensionality of substituted clusters, these should possess attractive properties as cross-linkers for existing classes of polymeric materials.[163]

Clusters exhibiting pseudo-metallic properties manifested in their photoredox properties also have many unexplored avenues. First, understanding how functionalization affects the redox chemistry and the radical states of these highly delocalized systems is fundamentally important. The physical properties associated with unpaired electrons of functionalized species need to be studied further, both in the solid and solution states. These species can provide an entry to a unique chemistry of stable radicals, which can be used as building blocks with strong magnetic coupling properties to design molecular magnets.[164] Furthermore, these molecules can potentially exhibit useful properties for spin labeling and nuclear polarization transfer.[165,166] Given the potential materials-favorable properties of many perfunctionalized redox-active boron clusters, we expect that these species can be used as charge carrier scaffolds with good stability, cyclability, and potentially enhanced voltage characteristics in devices including polymer-based and redox-flow batteries.[167,168] Likewise, the ability to control geometry and electronic delocalization between the cluster and tethered substituents should allow one to tune charge-transfer properties of the resulting systems and ultimately design metal-free chromophores with tunable absorption/emission colors and excited state lifetimes.

Perfunctionalized boron clusters can also be envisioned as building blocks for hierarchical hybrid materials. Recent developments in the field of hybrid porous solids[169] clearly showcase the need for rigid, tunable, and robust three-dimensional building blocks. Furthermore, atomically precise 3D hierarchical materials containing nano-sized building blocks can be also used for assembly of nanoparticles into hierarchical extended structures. For example, cluster-based molecules can be synthesized with a densely packed corona of

functional groups that will bind to the surface of nanoparticles. Tuning the aspect ratios of these clusters and nanoparticles may provide a method for creating assemblies with tunable plasmonic[170] and catalytic properties.[171]

Finally, in contrast to carbon-based aromatic building blocks where there exist numerous chemical transformations enabling the functionalization of C–H bonds, methods targeting heterofunctionalized boron clusters are still currently very limited. Metal-catalyzed transformations will likely emerge in the future targeting synthesis of these molecules.[172] Significantly, many opportunities can be envisioned that stem directly from the ability to generate complex structures that contain multiple functional groups appended to its vertices (*vide supra*). Beyond metal-based catalysis, several studies indicate that perhalogenated carboranes and boron clusters can undergo substitution at B–Cl and B–F vertices,[173,174] suggesting it should be possible to design more well-behaved reaction protocols for creating vertex-differentiated systems *via* this relatively unexplored pathway. We are strongly convinced that expanding a molecular toolbox of existing organic and hybrid monomers for polymer synthesis through introduction of new perfunctionalized boron-rich cluster architectures will create a fundamentally new class molecular materials.

Acknowledgments

Funding Sources

A.M.S. acknowledges the University of California, Los Angeles (UCLA) Department of Chemistry and Biochemistry for start-up funds, 3M for a Non-Tenured Faculty Award, the American Chemical Society Petroleum Research Fund (56562-DNI3) for the Doctoral New Investigator Grant, Alfred P. Sloan Foundation for Research Fellowship in Chemistry and NIGMS for the Maximizing Investigator's Research Award (R35GM124746). E.A.Q. is a recipient of a NIH Predoctoral Training Fellowship through the UCLA Chemistry-Biology Interface Training Program under the National Research Service Award (T32GM008496).

Authors thank Rafal M. Dziedzic for assistance with computational work.

References

1. Miyaura N, Suzuki A. Palladium-Catalyzed Cross-Coupling Reactions of Organoboron Compounds. Chem Rev. 1995; 95:2457–2483.
2. For details see: Spokoyny AM. New Ligand Platforms Featuring Boron-Rich Clusters as Organomimetic Substituents. Pure & Appl Chem. 2013; 85:903–919.
3. Crawford B Jr, Eberhardt WH, Lipscomb WN. The Valence Structure of the Boron Hydrides. J Chem Phys. 1954; 22:989–1001.
4. Longuet-Higgins HC, Roberts M, de V. The Electronic Structure of an Icosahedron of Boron Atoms. Proc R Soc London, Ser A. 1955; 230:110–119.
5. Pitochelli AR, Hawthorne MF. The Isolation of the Icosahedral $B_{12}H_{12}^{2-}$ Ion. J Am Chem Soc. 1960; 82:3228–3229.
6. Hawthorne MF, Pitochelli AR. The Reactions of Bis-Acetonitrile Decaborane with Amines. J Am Chem Soc. 1959; 81:5519–5519.
7. Hawthorne MF, Maderna A. Applications of Radiolabeled Boron Clusters to the Diagnosis and Treatment of Cancer. Chem Rev. 1999; 99:3421–3434. [PubMed: 11849026]
8. Valiant JF, Guenther KJ, King AS, Morel P, Schaffer P, Sogbein OO, Stephenson KA. The Medicinal Chemistry of Carboranes. Coord Chem Rev. 2002; 232:173–230.
9. Sivaev IB, Bregadze VI, Sjöberg S. Chemistry of *closo*-Dodecaborate Anion $B_{12}H_{12}^{2-}$: A Review. Collect Czech Chem Commun. 2002; 67:679–727.

10. Sivaev IB, Bregadze VI. Polyhedral Boranes for Medical Applications: Current Status and Perspectives. Eur J Inorg Chem. 2009:1433–1450.
11. Kaim W, Hosmane NS, Záliš S, Maguire JA, Lipscomb WN. Boron Atoms as Spin Carriers in Two- and Three-Dimensional Systems. Angew Chem, Int Ed. 2009; 48:5082–5091.
12. Issa F, Kassiou M, Rendina LM. Boron in Drug Discovery: Carboranes as Unique Pharmacophores in Biologically Active Compounds. Chem Rev. 2011; 111:5701–5722. [PubMed: 21718011]
13. Hosmane, NS. Boron Science: New Technologies and Applications. CRC Press; Boca Raton, FL: 2011.
14. Scholz M, Hey-Hawkins E. Carbaboranes as Pharmacophores: Properties, Synthesis, and Application Strategies. Chem Rev. 2011; 111:7035–7062. [PubMed: 21780840]
15. Grimes, RN. Carboranes. 3. Academic Press; 2016.
16. Olid D, Núñez R, Viñas C, Teixidor F. Methods to Produce B–C, B–P, B–N and B–S Bonds in Boron Clusters. Chem Soc Rev. 2013; 42:3318–3336. [PubMed: 23318646]
17. Douvris C, Michl J. Chemistry of the Carba-*closo*-Dodecaborate(-) Anion, $CB_{11}H_{12}^-$. Chem Rev. 2013; 113:PR179–PR233. [PubMed: 23944158]
18. Núñez R, Romero I, Teixidor F, Viñas C. Icosahedral Boron Clusters: A Perfect Tool for the Enhancement of Polymer Features. Chem Soc Rev. 2016; 45:5147–5173. [PubMed: 27188393]
19. Núñez R, Tarrés M, Ferrer-Ugalde A, Fabrizi de Biani F, Teixidor F. Electrochemistry and Photoluminescence of Icosahedral Carboranes, Boranes, Metallacarboranes, and Their Derivatives. Chem Rev. 2016; 116:14307–14378. [PubMed: 27960264]
20. Welch AJ. The Significance and Impact of Wade's Rules. Chem Commun. 2013; 49:3615–3616. (and references therein).
21. King RB. Three-Dimensional Aromaticity in Polyhedral Boranes and Related Molecules. Chem Rev. 2001; 101:1119–1152. [PubMed: 11710215]
22. Braunschweig H, Dewhurst RD. Single, Double, Triple Bonds and Chains: The Formation of Electron-Precise B–B Bonds. Angew Chem, Int Ed. 2013; 52:3574–3583.
23. Braunschweig H, Dewhurst RD, Mozo S. Bulding Electron-Precise Boron–Boron Single Bonds: Imposing Monogamy on a Promiscuous Element. ChemCatChem. 2015; 7:1630–1638.
24. For references, see: Davan T, Morrison JA. Chemistry of the Boron Subhalides: Preparation, Boron Nuclear Magnetic Resonance, and Thermal Stability of Tetraboron Tetrachloride. Inorg Chem. 1979; 18:3194–3197.
25. Urry G, Wartik T, Schlesinger HI. A New Sub-Chloride of Boron, B_4Cl_4. J Am Chem Soc. 1952; 74:5809–5809.
26. Ajoti A, Lipscomb WN. The Crystal and Molecular Structure of B_4Cl_4. Acta Crystallogr. 1953; 6:547–550.
27. Mennekes T, Paetzold P, Boese R, Bläser D. Tetra-*tert*-butyltetraboratetrahedrane. Angew Chem, Int Ed Engl. 1991; 30:173–175.
28. Hnyk D. T Symmetrical Gaseous Tetra-*tert*-butyltetrahoratetrahedrane: An Electron Diffraction Study. Polyhedron. 1997; 16:603–606.
29. Davan T, Morrison JA. Tetrakis(t-butyl)tetraborane(4), Bu4tB4; Synthesis of the First Peralkyl Derivative of a 2*N* Framework Electron Count Deltahedral Borane. J Chem Soc, Chem Comm. 1981:250–251.
30. B_4Cl_4 reactivity: Morrison JA. Chemistry of the Polyhedral Boron Halides and the Diboron Tetrahalides. Chem Rev. 1991; 91:35–48.
31. Maier CJ, Pritzkow H, Siebert W. Blue Tetrakis(diisopropylamino)-*cyclo*-tetraborane and Yellow Tetrakis(tetramethylpiperidino)tetraboratetrahedrane. Angew Chem, Int Ed. 1999; 38:1666–1668.
32. See ref. 2 in: Präsang C, Hofmann M, Geiseler G, Massa W, Berndt A. Topomerization of a Distorted Diamond-Shaped Tetraborane(4) and Its Hydroboration to a *closo*-Pentaborane(7) with a *nido* Structure. Angew Chem, Int Ed. 2003; 42:1049–1052.
33. Neu A, Mennekes T, Paetzold P, Englert U, Hofmann M, von Ragué Schleyer P. Novel Tetralkyltetraboranes of the Type B_4R_4, $B_4H_2R_4$ and $B_4H_4R_4$. Inorg Chim Acta. 1999; 289:58–69.

34. Preetz W, Peters G. The Hexahydro-*closo*-hexaborate Dianion $[B_6H_6]^{2-}$ and Its Derivatives. Eur J Inorg Chem. 1999:1831–1846.
35. Klandberg F, Muetterties EL. Chemistry of Boranes. XXVII. New Polyhedral Borane Anions, $B_9H_9^{2-}$ and $B_{11}H_{11}^{2-}$. Inorg Chem. 1966; 5:1955–1960.
36. Preetz W, Fritze J. Preparation, ^{11}B NMR and Vibrational Spectra of the Octahedral *closo*-Borate Anions $B_6X_6^{2-}$; X = H, Cl, Br, I. Z Naturforsch. 1984; 39b:1472–1477.
37. Fritze J, Preetz W, Marsmann HC. *closo*-Halogenohydrohexaborate, II ^{11}B NMR Spectra of the *closo*-Halogenohydrohexaborates $X_nB_6B_{6-n}^{2-}$, n = 0–6; X = Cl, Br, I. Z Naturforsch. 1987; 42b: 287–292.
38. Fritze J, Preetz W. *closo*-Halogenohydrohexaborate, III Vibrational Spectra of the closo-Halogenohydrohexaborates $X_nB_6B_{6-n}^{2-}$, n = 1–5; X = Cl, Br, I. Z Naturforsch. 1987; 42b:293–300.
39. Preetz W, Stallbaum M. Preparation and ^{11}B NMR Spectra of the Perhalogenated *closo*-Hexaborates $B_6X_nY_{6-n}^{2-}$, n = 0–6; X ≠ Y = Cl, Br, I. Z Naturforsch. 1990; 45b:1113–1117.
40. Thesing J, Stallbaum M, Preetz W. Vibrational Spectra and Noraml Coordinate Analysis of the Heteroleptic Halogenohexaborates $B_6X_nY_{6-n}^{2-}$, n = 1–5; X ≠ Y = Cl, Br, I. Z Naturforsch. 1991; 46b:602–608.
41. Baudler M, Rockstein K, Oehlert W. Tris(diethylamino)cyclotriborane and Constitutional Isomerism Between *cyclo*- and *closo*-Hexakis(diethylamino)hexaborane(6). Chem Ber. 1991; 124:1149–1152.
42. Siebert W, Maier CJ, Greiwe P, Bayer MJ, Jofmann M, Pritzkow H. Small Boranes, Carboranes, and Heterocarboranes. Pure Appl Chem. 2003; 75:1277–1286.
43. Mesbah W, Soleimani M, Kianfar E, Geiseler G, Massa W, Hofmann M, Berndt A. *hypercloso*-Hexa(amino)hexaboranes: Structurally Related to Known *hypercloso*-Dodecaboranes, Metastable with Regard to Their Classical Cycloisomers. Eur J Inorg Chem. 2009:5577–5582.
44. Wixtrom AI, Shao Y, Jung D, Machan CW, Kevork SN, Qian EA, Axtell JC, Khan SI, Kubiak CP, Spokoyny AM. Rapid Synthesis of Redox-Active Dodecaborane $B_{12}(OR)_{12}$ Clusters under Ambient Conditions. Inorg Chem Front. 2016; 3:711–717. [PubMed: 27885335]
45. Qian EA, Wixtrom AI, Axtell JC, Saebi A, Jung D, Rehak P, Han Y, Moully EH, Mosallaei D, Chow S, Messina MS, Wang JY, Royappa AT, Rheingold AL, Maynard HD, Král P, Spokoyny AM. Atomically Precise Organomimetic Cluster Nanomolecules Assembled *via* Perfluoroaryl-Thiol S_NAr Chemistry. Nature Chem. 2017; 9:333–340. [PubMed: 28485398]
46. Messina MS, Axtell JC, Wang Y, Chong P, Wixtrom AI, Kirlikovali KO, Upton BM, Hunter BM, Shafaat OS, Khan SI, Winkler JR, Gray HB, Alexandrova AN, Maynard HD, Spokoyny AM. Visible-Light-Induced Olefin Activation Using 3D Aromatic Boron-Rich Cluster Photooxidants. J Am Chem Soc. 2016; 138:6952–6955. [PubMed: 27186856]
47. Bykov AY, Zhdanov AP, Zhizhin KY, Kuznetsov NT. Structure, Physicochemical Properties, and Reactivity of the $[B_9H_9]^{2-}$ Anion. Russ J Inorg Chem. 2016; 61:1629–1648.
48. Klanberg F, Eaton DR, Guggenberger LJ, Muetterties EL. Chemistry of Boranes. XXVIII. New Polyhedral Borane Anions, $B_8H_8^{2-}$, $B_8H_8^{\cdot-}$, and $B_7H_7^{2-}$. Inorg Chem. 1967; 6:1271–1281.
49. Knoth WH, Miller HC, England DC, Parshall GW, Muetterties EL. Derivative Chemistry of $B_{10}H_{10}^{-}$ and $B_{12}H_{12}^{-}$. J Am Chem Soc. 1962; 84:1056–1057.
50. Hoffmann R, Lipscomb WN. Sequential Substitution Reactions on $B_{10}H_{10}^{-2}$ and $B_{12}H_{12}^{-2}$. J Chem Phys. 1962; 37:520–523.
51. Hertler WR, Raasch MS. Chemistry of Boranes. XIV. Amination of $B_{10}H_{10}^{-2}$ and $B_{12}H_{12}^{-2}$ with Hydroxalamine-*O*-Sulfonic Acid. J Am Chem Soc. 1964; 86:3661–3668.
52. Muetterties EL, Balthis JH, Chia YT, Knoth WH, Miller HC. Chemistry of Boranes. VIII. Salts and Acids of $B_{10}H_{10}^{-2}$ and $B_{12}H_{12}^{-2}$. Inorg Chem. 1964; 3:444–451.
53. Knoth WH, Miller HC, Sauer JC, Balthis JH, Chia YT, Muetterties EL. Chemistry of Boranes. IX. Halogenation of $B_{10}H_{10}^{-2}$ and $B_{12}H_{12}^{-2}$. Inorg Chem. 1964; 3:159–167.
54. Sivaev IB, Prikaznov AV, Naoufal D. Fifty Years of the *closo*-Decaborate Anion Chemistry. Collect Czechoslov Chem Commun. 2010; 75:1149–1199.
55. Kutz NA, Morrison JA. 2*N* Framework Electron Clusters: Proparation and Relative Thermal Stabilitites of the Polyhedran Boron Subbromides. Inorg Chem. 1980; 19:3295–3299.

56. Gielen M. Does the Valence State Index Reflect the Stabililty of Neutral Boron Subhalide Clusters? Theor Chim Acta. 1982; 61:21–28.
57. Hönle W, Grin Y, Burkhardt A, Wedig U, Schultheiss M, von Schnering HG, Kellner R, Binder H. Syntheses, Crystal Structures, and Electronic Structure of the Boron Halides B_9X_9 (X = Cl, Br, I). J Solid State Chem. 1997; 133:59–67.
58. Speiser B, Wizemann T, Würde M. Two-Electron-Transfer Redox Systems Part 7: Two-Step Electrochemical Oxidation of the Boron Subhalide Cluster Dianions $B_6X_6^{2-}$ (X = Cl, Br, I). Inorg Chem. 2003; 42:4018–4028. [PubMed: 12817957]
59. Kabbani RM, Wong EH. Selective Synthesis of the Nonachlorononaborate Clusters B_9Cl_9 and $B_9Cl_9^{2-}$. J Chem Soc Chem Commun. 1978:462–463.
60. Emery SL, Morrison JA. 2*n* Framework Electron Clusters: Directed Synthesis of Octachlorooctaborane, B_8Cl_8. The Activation of Carbon-Hydrogen Bonds. J Am Chem Soc. 1982; 104:6790–6791.
61. Volkov O, Dirk W, Englert U, Paetzold P. Undecaborates $M_2[B_{11}H_{11}]$: Facile Synthesis, Crystal Structure, and Reactions. Z Anorg Allg Chem. 1999; 625:1193–1200.
62. Schlüter F, Bernhardt E. Syntheses and Crystal Structures of the *closo*-Borates $M_2[B_7H_7]$ and $M[B_7H_8]$ (M = PPh_4, PNP, and N(*n*-Bu_4)): the Missing Crystal Structure in the Series $[B_nH_n]^{2-}$ (*n* = 6 – 12). Inorg Chem. 2011; 50:2580–2589. [PubMed: 21341737]
63. Schlüter F, Bernhardt E. Syntheses and Crystal Structures of the *closo*-Borate $M[B_8H_9]$ (M = $[PPh_4]^+$ and $[N(n\text{-}Bu_4)]^+$). Inorg Chem. 2012; 51:511–517. [PubMed: 22136316]
64. Zhizhin KY, Zhdanov AP, Kuznetsov NT. Derivatives of *closo*-Decaborate Anion $[B_{10}H_{10}]^{2-}$ with *exo*-Polyhedral Substituents. Russ J Inorg Chem. 2010; 55:2089–2127.
65. Gu X, Ozerov OV. Exhaustive Chlorination of $[B_{12}H_{12}]^{2-}$ without Chlorine Gas and the Use of $[B_{12}Cl_{12}]^{2-}$ as a Supporting Anion in Catalytic Hydrodefluorination of Aliphatic C–F Bonds. Inorg Chem. 2011; 50:2726–2728. [PubMed: 21361302]
66. Solntsev KA, Mebel AM, Votinova NA, Kuznetsov NT, Charkin OP. Dodecahydrododecaborate(2-) Polyhedral Anion as a Spacial Aromatic System. Koord Khim. 1992; 18:340–364.
67. Ivanov SV, Miller SM, Anderson OP, Solntsev KA, Strauss SH. Synthesis and Stability of Reactive Salts of Dodecafluoro-*closo*-dodecaborate(2-). J Am Chem Soc. 2003; 125:4694–4695. [PubMed: 12696872]
68. Peryshkov DV, Popov AA, Strauss SH. Direct Perfluorination of $K_2B_{12}H_{12}$ in acetonitrile Occurs at the Gas Bubble-Solution Interface and Is Inhibited by HF. Experimental and DFT Study of Inhibition by Protic Acids and Soft, Polarizable Anions. J Am Chem Soc. 2009; 131:18393–18403. [PubMed: 19954188]
69. Peymann T, Herzog A, Knobler CB, Hawthorne MF. Aromatic Polyhedral Hydroxyborates: Briding Boron Oxides and Boron Hydrides. Angew Chem, Int Ed. 1999; 38:1061–1064.
70. Peymann T, Knobler CB, Khan SI, Hawthorne MF. Dodecahydroxy-*closo*-dodecaborate(2-). J Am Chem Soc. 2001; 123:2182–2185. [PubMed: 11456863]
71. Farha OK, Julius RL, Lee MW, Huertas RE, Knobler CB, Hawthorne MF. Synthesis of Stable Dodecaalkoxy Derivatives of *hypercloso*-$B_{12}H_{12}$. J Am Chem Soc. 2005; 127:18243–18251. [PubMed: 16366578]
72. Maderna A, Knobler CB, Hawthorne MF. Twelvefold Functionalization of an Icosahedral Surface by Total Esterification of $[B_{12}(OH)_{12}]^{2-}$: 12(12)-Closomers. Angew Chem, Int Ed. 2001; 40:1661–1664.
73. Thomas J, Hawthorne MF. Dodeca(carboranyl)-Substituted Closomers: Toward Unimolecular Nanoparticles as Delivery Vehicles for BNCT. Chem Commun. 2001:1884–1885.
74. Li T, Jalisatgi SS, Bayer MJ, Maderna A, Khan SI, Hawthorne MF. Organic Syntheses on an Icosahedral Borane Surface: Closomer Structures with Twelvefold Functionality. J Am Chem Soc. 2005; 127:17832–17841. [PubMed: 16351114]
75. Peymann T, Knobler CB, Khan SI, Hawthorne MF. Dodeca(benzyloxy)dodecaborane, $B_{12}(OCH_2Ph)_{12}$: A Stable Derivative of *hypercloso*-$B_{12}H_{12}$. Angew Chem, Int Ed. 2001; 40:1664–1667.

76. Miller EC, Hertler WR, Muetterties EL, Knoth WH, Miller NE. Chemistry of Boranes. XXV. Synthesis and Chemistry of Base Derivatives of $B_{10}H_{10}^{2-}$ and $B_{12}H_{12}^{2-}$. Inorg Chem. 1965; 4:1216–1221.
77. Ivanov SV, Davis JA, Miller SM, Anderson OP, Strauss SH. Synthesis and Characterization of Ammonioundecafluoro-*closo*-dodecaborates(1-). New Superweak Anions. Inorg Chem. 2003; 42:4489–4491. [PubMed: 12870929]
78. Bolli C, Derendorf J, Jenne C, Scherer H, Sindlinger CP, Wegener B. Synthesis and Properties of the Weakly Coordinating Anion $[Me_3NB_{12}Cl_{11}]$. Chem Eur J. 2014; 20:13783–13792. [PubMed: 25196859]
79. Zhang Y, Liu J, Duttwyler S. Synthesis and Structural Characterization of Ammonio/Hydroxo Undecachloro-*closo*-Dodecaborates $[B_{12}Cl_{11}NH_3]^-$/$[B_{12}Cl_{11}OH]^{2-}$ and Their Derivatives. Eur J Inorg Chem. 2015:5158–5162.
80. Peymann T, Knobler CB, Hawthorne MF. An Icosahedral Array of Methyl Groups Supported by an Aromatic Borane Scaffold: The $[closo\text{-}B_{12}(CH_3)_{12}]^{2-}$ Ion. J Am Chem Soc. 1999; 121:5601–5602.
81. Bondarev O, Hawthorne MF. Catalytic Hydroxylation of $[Closo\text{-}B_{12}H_{12}]^{2-}$ – Adaptation of the Periana Reaction to a Polyhedral Borane. Chem Commun. 2011; 47:6978–6980.
82. Jalisatgi SS, Kulkarni VS, Tang B, Houston ZH, Lee MW, Hawthorne MF. A Convenient Route to Diversely Substituted Icosahedral Closomer Nanoscaffolds. J Am Chem Soc. 2011; 133:12382–12385. [PubMed: 21766843]
83. Jenne C, Kirsch C. Alkoxy Substituted Halogenated *closo*-Dodecaborates as Anions for Ionic Liquids. Dalton Trans. 2015; 44:13119–13124. [PubMed: 26107425]
84. Bondarev O, Khan AA, Tu X, Sevryugina YV, Jalisatgi SS, Hawthorne MF. Synthesis of $[closo\text{-}B_{12}(OH)_{11}NH_3]^-$: A New Heterobifunctional Dodecaborane Scaffold for Drug Delivery Applications. J Am Chem Soc. 2013; 135:13204–13211. [PubMed: 23919884]
85. Heinrich A, Keller HL, Preetz W. Oxidation Reactions on $X_nB_6H_{6-n}^{2-}$, X = Cl, Br, I; $n = 1 – 6$: and Crystal Structures of $[(n\text{-}C_4H_9)_4N]B_6I_6$ and $[(n\text{-}C_4H_9)_4N]_2B_6I_6$. Z Naturforsch. 1990; 45b: 184–190.
86. Lorenzen V, Preetz W. Crystal Structures of $(n\text{-}Bu_4N)[B_6Cl_6]$, $(n\text{-}Bu_4N)[B_6Br_6]$, and $(Ph_3P{=}N{=}PPh_3)[B_6I_6]$, and Vibrational Spectra and Normal Coordinate Analysis of the Hexahalogeno-*closo*-hexaborate Radical Anions $[B_6X_6]^-$, X = Cl, Br. I. Z Naturforsch. 1997; 52b: 565–572.
87. Binder H, Kellner R, Vaas K, Hein M, Baumann F, Wanner M, Winter R, Kaim W, Hönle W, Grin Y, Wedig U, Schultheiss M, Kremer RK, von Schnering HG, Groeger O, Engelhardt G. The closo-Cluster Triad: B_9X_9, $[B_9X_9]^{\cdot -}$, and $[B_9X_9]^{2-}$ with Tricapped Trigonal Prisms (X = Cl, Br, I). Syntheses, Crystal and Electronic Structures. Z Anorg Allg Chem. 1999; 625:1059–1072.
88. Boeré RT, Derendorf J, Jenne C, Kacprzak S, Keßler M, Riebau R, Riedel S, Roemmele TL, Rühle M, Scherer H, Vent-Schmidt T, Warneke J, Weber S. On the Oxidation of the Three-Dimensional Aromatics $[B_{12}X_{12}]^{2-}$ (X = F, Cl, Br, I). Chem Eur J. 2014; 20:4447–4459. [PubMed: 24595990]
89. Wiersema RJ, Middaugh RL. Electrochemical Preparation and halogenation of 1,1′-μ-Hydro-bis(undecahydro-*closo*-dodecaborate)(3-), $B_{24}H_{23}^{3-}$. Inorg Chem. 1969; 8:2074–2079.
90. Rupich MW, Foos JS, Brummer SB. Characterization of Chloroclosoborane Acids as Electrolytes for Acid Fuel Cells. J Electrochem Soc. 1985; 132:119–122.
91. Boeré RT, Kacprzak S, Keßler M, Knapp C, Riebau R, Riedel S, Roemmele TL, Rühle M, Scherer H, Weber S. Oxidation of *closo*-$[B_{12}Cl_{12}]^{2-}$ to the Radical Anion $[B_{12}Cl_{12}]^{\cdot -}$ and to Neutral $B_{12}Cl_{12}$. Angew Chem, Int Ed. 2011; 50:549–552.
92. Van N, Tiritiris I, Winter RF, Sarkar B, Singh P, Duboc C, Muñoz-Castro A, Arratia-Pérez R, Kaim W, Schleid T. Oxidative Perhydroxylation of $[closo\text{-}B_{12}H_{12}]^{2-}$ to the Stable Inorganic Cluster Redox System $[B_{12}(OH)_{12}]^{2-/\cdot -}$: Experiment and Theory. Chem Eur J. 2010; 16:11242–11245. [PubMed: 20726020]
93. Peymann T, Knobler CB, Hawthorne MF. An Unpaired Electron Incarcerated with an Icosahedral Borane Cage: Syntehsis and Crystal Structure of the Blue, Air-Stable $\{[closo\text{-}B_{12}(CH_3)_{12}].\}^-$ Radical. Chem Commun. 1999:2039–2040.

94. Lee MW, Farha OK, Hawthorne MF, Hansch CH. Alkoxy Derivatives of Dodecaborate: Discrete Nanomolecular Ions with Tunable Pseudometallic Properties. Angew Chem, Int Ed. 2007; 46:3018–3022.
95. Hansch C, Leo A, Taft RW. A Survey of Hamett Substituent Constances and Resonance and Field Parameters. Chem Rev. 1991; 91:165–195.
96. Douvris C, Ozerov OV. Hydrodefluorination of Perfluoroalkyl Groups Using Silylium-Carborane Catalysts. Science. 2008; 321:1188–1190. [PubMed: 18755971]
97. Shao B, Bagdasarian AL, Popov S, Nelson HM. Arylation of Hydrocarbons Enabled by Organosilicon Reagents and Weakly Coordinating Anions. Science. 2017; 355:1403–1407. [PubMed: 28360325]
98. Kostjuk SV. Recent Progress in the Lewis Acid Co-Initiated Cationic Polymerization of Isobutylene and 1,3-Dienes. RSC Adv. 2015; 5:13125–13144.
99. Wegener M, Huber F, Bolli C, Jenne C, Kirsch SF. Silver-Free Activation of Ligated Gold(I) Chlorides: The Use of $[Me_3NB_{12}Cl_{11}]$ as a Weakly Coordinating Anion in Homogeneous Gold Catalysis. Chem Eur J. 2015; 21:1328–1336. [PubMed: 25394284]
100. Konze WV, Scott BL, Kubas GJ. First Example of B–C Bond Cleavage in the BAr_F ($B[C_6H_3(CF_3)_2$-3,5$]_4$) Anion Mediated by a Transition Metal Species, *trans*-$[(Ph_3P)_2Pt(Me)(OEt_2)]^+$ Chem Commun. 1999:1807–1808.
101. Salem H, Shimon LJW, Leitus G, Weiner L, Milstein D. B–C Bond Cleavage of BAr_F Anion Upon Oxidation of Rhodium(I) with $AgBAr_F$. Phosphinite Rhodium(I), Rhodium(II), and Rhodium(III) Pincer Complexes. Organometallics. 2008; 27:2293–2299.
102. Weber SG, Zahner D, Rominger F, Straub BF. A Cationic Gold Complex Cleaves $BArF_{24}$. Chem Commun. 2012; 48:11325–11327.
103. Bolli C, Derendorf J, Keßler M, Knapp C, Scherer H, Schulz C, Warneke J. Synthesis, Crystal Structure, and Reactivity of the Strongly Methylating Agent $Me_2B_{12}Cl_{12}$. Angew Chem Int Ed. 2010; 49:3536–2528.
104. Kessler M, Knapp C, Zogaj A. Cationic Dialkyl Metal Compounds of Group 13 Elements (E = Al, Ga, In) Stabilized by the Weakly Coordinating Dianion $[B_{12}Cl_{12}]^{2-}$. Organometallics. 2011; 30:3786–3792.
105. Saleh M, Powell DR, Wehmschulte RJ. Chlorination of 1-Carba-*closo*-dodecaborate and 1-Ammonio-*closo*-dodecaborate Anions. Inorg Chem. 2016; 55:10617–10627.
106. Avelar A, Tham FS, Reed CA. Superacidity of Boron Acids $H_2(B_{12}X_{12})$ (X = Cl, Br). Angew Chem Int Ed. 2009; 48:3491–3493.
107. Jenne C, Keßler M, Warneke J. Protic Anions $[H(B_{12}X_{12})]^-$ That Act as Brønsted Acids in the Gas Phase. Chem Eur J. 2015; 21:5887–5891. [PubMed: 25735766]
108. Lipping L, Leito I, Koppel I, Krossing I, Himmel D, Koppel IA. Superacidity of *closo*-Dodecaborate-Based Brønsted Acids: a DFT Study. J Phys Chem A. 2015; 119:735–743. [PubMed: 25513897]
109. Rogers RD, Sneddon KR. Ionic Liquids – Solvents of the Future? Science. 2003; 302:792–793. [PubMed: 14593156]
110. Bertocco P, Derendorf J, Jenne C, Kirsch C. Improving the Solubility of 1-Ammonio-*closo*-dodecaborate Anions. Inorg Chem. 2017; 56:3459–3466. [PubMed: 28240900]
111. Johnson JW, Brody JF. Lithium Closoborane Electrolytes: III. Preparation and Characterization. J Electrochem Soc. 1982; 129:2213–2219.
112. Dey AN, Miller J. Primary Li/$SOCl_2$ Cells: VII. Effect of $Li_2B_{10}Cl_{10}$ and $Li_2B_{12}Cl_{12}$ Electrolyte Salts on the Performance. J Electrochem Soc. 1979; 126:1445–1451.
113. Johnson JW, Whittingham MS. Lithium Closoboranes as Electrolytes in Solid Cathode Lithium Cells. J Electrochem Soc. 1980; 127:1653–1654.
114. Johnson JW, Thompson AH. Lithium Closoboranes II. Stable Nonaqueous Electrolytes for Elevated Temperature Lithium Cells. J Electrochem Soc. 1981; 128:932–933.
115. GirishKumar G, Bailey WH III, Peterson BK, Casteel WJ Jr. Electrochemical and Spectroscopic Investigations of the Overcharge Behavior of StabiLife Electrolyte Salts in Lithium-Ion Batteries. J Electrochem Soc. 2011; 158:A146–A153.

116. Ionica-Bousquet CM, Muñoz-Rojas D, Casteel WJ, Pearlstein RM, GirishKumar G, Pez GP, Palacín MR. Polyfluorinated Boron Cluster-Based Salts: A New Electrolyte for Application in $Li_4Ti_5O_{12}$/$LiMn_2O_4$ Rechargeable Lithium-Ion Batteries. J Power Sources. 2010; 195:1479–1485.
117. Stasko DJ, Perzynski KJ, Wasil MA, Brodbeck JK, Kirschbaum K, Kim YW, Lind C. An Addition to the Oxoacid Family: $H_2B_{12}(OH)_{12}$. Inorg Chem. 2004; 43:3786–3788. [PubMed: 15206854]
118. Bukovsky EV, Peryshkov DV, Wu H, Zhou W, Tang WS, Jones WM, Stavila V, Udovic TJ, Strauss SH. Comparison of the Coordination of $B_{12}F_{12}^{2-}$, $B_{12}Cl_{12}^{2-}$, and $B_{12}H_{12}^{2-}$ to Na+ in the Solid State: Crystal Structures and Thermal Behavior of $Na_2(B_{12}F_{12})$, $Na_2(H_2O)_4(B_{12}F_{12})$, $Na_2(B_{12}Cl_{12})$, and $Na_2(H_2O)_6(B_{12}Cl_{12})$. Inorg Chem. 2017; 56:4369–4379. [PubMed: 28383911]
119. Hawthorne MF. The Role of Chemistry in the Development of Boron Neutron Capture Therapy of Cancer. Angew Chem, Int Ed Engl. 1993; 32:950–984.
120. Wsek J. Potential Applications of the Boron Cluster Compounds. Chem Rev. 1992; 92:269–278.
121. Grimes RN. Boron Clusters Come of Age. J Chem Educ. 2004; 81:657–672.
122. Locher GL. Bioloical Effects and Therapeutic Possibilties of Netrons. Am J Roentgenol Radium Therapy. 1936; 36:1–13.
123. Hawthorne MF. New Horizons for Therapy Based on the Boron Neutraon Capture Reaction. Mol Med Today. 1998; 4:174–181. [PubMed: 9572059]
124. Moss RL. Critical Review, with an Optimistic Outlook, on Boron Neutron Capture Therapy (BNCT). Appl Radiat Isotopes. 2014; 88:2–11.
125. Slatkin DN. A History of Boron Netron Capture Therapy of Brain Tumours: Postulation of a Brain radiation Dose Tolerance Limit. Brain. 1991; 114:1609–1629. [PubMed: 1884169]
126. Lipscomb WN, Pitochelli AR, Hawthorne MF. Probable Structure of the $B_{10}H_{10}^{2-}$ Ion. J Am Chem Soc. 1959; 81:5833–5834.
127. Asbury AK, Ojemann RG, Nielsen SL. Neuropathologic Study of Fourteen Cases of Malignant Brain Tumor Treated by Boron-10 Slow Neutron Capture Radiation. J Neuropathol Exp Neurol. 1972; 31:278–303. [PubMed: 4337274]
128. Barth RF, Soloway AH, Fairchild RG, Brugger RM. Boron Neutron Capture Therapy for Cancer. Realities and Prospects. Cancer. 1992; 70:2995–3007. [PubMed: 1451084]
129. Soloway AH, Hatanaka H, Davis MA. Penetration of Brain and Brain Tumor. VII. Tumor-Binding Sulfhydryl Boron Compounds. J Med Chem. 1967; 10:714–717. [PubMed: 6037065]
130. Ciani L, Ristori S. Boron as a Platform for New Drug Design. Expert Opin Drug Discov. 2012; 7:1017–1027. [PubMed: 22946655]
131. Barth RF, Coderre JA, Vicente MGH, Blue TE. Boron Neutron Capture Therapy of Cancer: Current Status and Future Prospects. Clin Cancer Res. 2005; 11:3987–4002. [PubMed: 15930333]
132. Nakamura, H., Kirihata, M. Neutron Capture Therapy. Sauerwein, W.Wittig, A.Moss, R., Nakagawa, Y., editors. Springer Berlin Heidelberg; Berlin, Heidelberg: 2012.
133. Soloway AH, Tjarks W, Barnum BA, Rong FG, Barth RF, Codogni IM, Wilson JG. The Chemistry of Neutron Capture Therapy. Chem Rev. 1998; 98:1515–1562. [PubMed: 11848941]
134. Sumitani S, Nagasaki Y. Boron Neutron Capture Therapy Assisted by Boron-Conjugated Nanoparticles. Polym J. 2012; 44:522–530.
135. Zhu YZ, Lin Y, Zhu YZ, Lu J, Maguire JA, Hosmane NS. Boron Drug Delivery *via* Encapsulated Magnetic Nanocomposites: A New Approach for BNCT in Cancer Treatment. J Nanomater. 2010; 2010:1–8.
136. Mandal S, Bakeine GJ, Krol S, Ferrari C, Clerici AM, Zonta C, Cansolino L, Ballarini F, Bortolussi S, Stella S, Protti N, Bruschi P, Altieri S. Design, Development, and Characterization of Multi-Functional Gold Nanoparticles for Biodetection and Targeted Boron Delivery in BNCT Applications. Appl Radiat Isotopes. 2011; 69:1692–1697.
137. Umano M, Uechi K, Uriuda T, Murayama S, Azuma H, Shinohara A, Liu Y, Ono K, Kirihata M, Yanagie H, Nagasaki T. Tumor Accumulation of ε-poly-lysines-based Polyamines Conjugated with Boron Clusters. Appl Radiat Isotopes. 2011; 69:1765–1767.

138. Yanagië H, Tomita T, Kobayashi H, Fujii Y, Takahashi T, Hasumi K, Nariuchi H, Sekiguchi M. Application of Boronated Anti-CEA Immunoliposome to Tumour Cell Growth Inhibition in *in* vitro Boron Neutron Capture Therapy Model. Br J Cancer. 1991; 63:522–526. [PubMed: 2021537]
139. Shelly K, Feakes DA, Hawthorne MF, Schmidt PG, Krisch TA, Bauer WF. Model Studies Directed Toward the Boron Neutron-Capture Therapy of Cancer: Boron Delivery to Murine Tumors with Liposomes. Proc Natl Acad Sci US A. 1992; 89:9039–9043.
140. Pan XQ, Wang H, Shukla S, Sekido M, Adams DM, Tjarks W, Barth RF, Lee RJ. Boron-Containing Folate Receptor-Targeted Liposomes as Potential Delivery Agents for Neutron Capture Therapy. Bioconjug Chem. 2002; 13:435–442. [PubMed: 12009931]
141. Maruyama K, Ishida O, Kasaoka S, Takizawa T, Utoguchi N, Shinohara A, Chiba M, Kobayashi H, Eriguchi M, Yanagie H. Intracellular Targeting of Sodium Mercaptoundecahydrododecaborate (BSH) to Solid Tumors by Transferrin-PEG Liposomes, for Boron Neutron-Capture Therapy (BNCT). J Control Release. 2004; 98:195–207. [PubMed: 15262412]
142. Feakes DA, Shelly K, Hawthorne MF. Selective Boron Delivery to Murine Tumors by Lipophilic Species Incorporated in the membranes of Unilamellar Liposomes. Proc Natl Acad Sci US A. 1995; 92:1367–1370.
143. Hawthorne MF, Shelly K. Liposomes as Drug Delivery Vehicles for Boron Agents. J Neurooncol. 1997; 33:53–58. [PubMed: 9151223]
144. Feakes DA, Spinler JK, Harris FR. Synthesis of Boron-Containing Cholesterol Derivatives for Incorporation into Unilamellar Liposomes and Evaluation as Potential Agents for BNCT. Tetrahedron. 1999; 55:11177–11186.
145. Lee JD, Ueno M, Miyajima Y, Nakamura H. Synthesis of Boron Cluster Lipids: *closo*-Dodecaborate as an Alternative Hydrophilic Function of Boronated Liposomes for Neutron Capture Therapy. Org Lett. 2007; 9:323–326. [PubMed: 17217295]
146. Heber EM, Hawthorne MF, Kueffer PJ, Garabalino MA, Thorp SI, Pozzi ECC, Hughes AM, Maitz CA, Jalisatgi SS, Nigg DW, Curotto P, Trivillin VA, Schwint AE. Therapeutic Efficacy of Boron Neutron Capture Therapy Mediated by Boron-Rich Liposomes for Oral Cancer in the Hamster Cheek Pouch Model. Proc Natl Acad Sci. 2014; 111:16077–16081. [PubMed: 25349432]
147. Ma L, Hamdi J, Wong F, Hawthorne MF. Closomers of High Boron Content: Synthesis, Characterization, and Potential Application as Unimolecular Nanoparticle Delivery Vehicles for Boron Neutron Capture Therapy. Inorg Chem. 2006; 45:278–285. [PubMed: 16390066]
148. Kuperman MV, Losytskyy MY, Bykov AY, Yarmoluk SM, Zhizhin KY, Kuznetsov NT, Varzatskii OA, Gumienna-Kontecka E, Kovalska VB. Effective Binding of Perhalogenated *closo*-Borates to Serum Albumins Revealed by Spectroscopic and ITC Studies. J Mol Struct. 2017; 1141:75–80.
149. Losytskyy MY, Kovalska VB, Varzatskii OA, Kuperman MV, Potocki S, Gumienna-Kontecka E, Zhdanov AP, Yarmoluk SM, Voloshin YZ, Zhizhin KY, Kuznetsov NT, Elskaya AV. An Interaction of the Functionalized closo-Borates with Albumins: The Protein Fluorescence Quencing and Calorimetry Study. J Luminescence. 2016; 169:51–60.
150. Sarma SJ, Khan AA, Goswami LN, Jalisatgi SS, Hawthorne MF. A Trimodal Closomer Drug-Delivery System Tailored with Tracing and Targeting Capabilities. Chem Eur J. 2016; 22:12715–12723. [PubMed: 27416332]
151. Pushechnikov A, Jalisatgi SS, Hawthorne MF. Dendritic Closomers: Novel Spherical Hybrid Dendrimers. Chem Commun. 2013; 49:3579–3581.
152. Kojima C, Kono K, Maruyama K, Takagishi T. Synthesis of Polyamidoamine Dendrimers Having Poly(ethylene glycol) Grafts and Their Ability to Encapsulate Anticancer Drugs. Bioconjug Chem. 2000; 11:910–917. [PubMed: 11087341]
153. Armstrong AF, Valliant JF. The Bioinorganic and Medicinal Chemistry of Carboranes: From New Drug Discovery to Molecular Imaging and Therapy. Dalton Trans. 2007; 38:4240–4251.
154. Goswami LN, Ma L, Chakravarty S, Cai Q, Jalisatgi SS, Hawthorne MF. Discrete Nanomolecular Polyhedral Borane Scaffold Supporting Multiple Gadolinium(III) Complexes as a High Performance MRI Contrast Agent. Inorg Chem. 2013; 52:1694–1700. [PubMed: 23126285]

155. Caravan P. Protein-Targeted Gadolinium-Based Magnetic Resonance Imaging (MRI) Contrast Agents: Design and Mechanism of Action. Acc Chem Res. 2009; 42:851–862. [PubMed: 19222207]
156. Langereis S, de Lussanet QG, van Genderen MHP, Backes WH, Meijer EW. Multivalent Contrast Agents Based on Gadolinium-Diethylenetriaminepentaacetic Acid-Terminated Poly(propylene imine) Dendrimers for Magnetic Resonance Imaging. Macromolecules. 2004; 37:3084–3091.
157. Goswami LN, Ma L, Cai Q, Sarma SJ, Jalisatgi SS, Hawthorne MF. cRGD Peptide-Conjugated Icosahedral *closo*-B_{12}^{2-} Core Carrying Multiple Gd^{3+}-DOTA Chelates for $\alpha_v\beta_3$ Integrin-Targeted Tumor Imaging (MRI). Inorg Chem. 2013; 52:1701–1709. [PubMed: 23391150]
158. Graham, B. Polymers Derived from Metal Decaborates and Dodecaborates. US Patent. 3368878. Feb 13, 1968
159. Schaefgen JR, Miller HC, Sauer JC, Sharkey WH. Polymers Containing Polyhedral Borane Rings I. Condensation Polymers. Journal of Polymer Science Part A-1: Polymer Chemistry. 1971; 9:51–68.
160. Spokoyny AM, Farha OK, Mulfort KL, Hupp JT, Mirkin CA. Porosity Tuning of Carborane-Based Metal-Organic Frameworks (MOFs) *via* Coordination Chemistry and Ligand Design. Inorg Chim Acta. 2011; 364:266–271.
161. Arata, K. Preparation of Superacidic Metal Oxides and Their Catalytic Action. In: Jackson, SD., Hargreaves, JSJ., editors. Metal Oxide Catalysis. Wiley-VCH; Weinheim, Germany: 2009.
162. Mortimer DA. Synthetic Polyelectrolytes – A Review. Polym Int. 1991; 25:29–41.
163. Zhou N, Cao Z, Xu B. Functional Hyper-Crosslinkers. Chem Eur J. 2017; 23:15844–15851. [PubMed: 28881458]
164. DeGayner JA, Jeon IR, Sun L, Dinca M, Harris TD. 2D Conductive Iron-Quinoid Magnets Ordering up to T_c = 105K *via* Heterogenous Redox Chemistry. J Am Chem Soc. 2017; 139:4175–4184. [PubMed: 28230984]
165. Michaelis VK, Smith AA, Corzilius B, Haze O, Swager TM, Griffin RG. High-Field ^{13}C Dynamic Nuclear Polarization with a Radical Mixture. J Am Chem Soc. 2013; 135:2935–2938. [PubMed: 23373472]
166. Jagtap AP, Krstic I, Kunjir NC, Hänsel R, Prisner TF, Sigurdsson ST. Sterically Shielded Spin Labels for In-Cell EPR Spectroscopy: Analysis of Stability in Reducing Environment. Free Radic Res. 2015; 49:78–85. [PubMed: 25348344]
167. Nishide H, Oyaizu K. Toward Flexible Batteries. Science. 2008; 319:737–738. [PubMed: 18258887]
168. Dmello R, Milshtein JD, Brushett FR, Smith KC. Cost-Driven Materials Selection Criteria for Redox Flow Battery Electrolytes. J Power Sources. 2016; 330:261–272.
169. Popp TMO, Yaghi OM. Sequence-Dependent Materials. Acc Chem Res. 2017; 50:532–534. [PubMed: 28945416]
170. Jones MR, Osberg KD, MacFarlane RJ, Langille MR, Mirkin CA. Templated Techniques for the Synthesis and Assembly of Plasmonic Nanostructures. Chem Rev. 2011; 111:3736–3827. [PubMed: 21648955]
171. Auyeung E, Morris W, Mondloch JE, Hupp JT, Farha OK, Mirkin CA. Controlling Structure and Porosity in Catalytic nanoparticle Superlattices with DNA. J Am Chem Soc. 2015; 137:1658–1662. [PubMed: 25611764]
172. Zhang Y, Sun Y, Lin F, Liu J, Duttwyler S. Rhodium(III)-Catalyzed Alkynylation-Annulation of *closo*-Dodecaborate Anions through Double B–H Activation at Room Temperature. Angew Chem. 2016; 128:15838–15843.
173. Fajardo J Jr, Chan AL, Tham FS, Lavallo V. Synthesis and Characterization of Anionic Polybrominated Carboranyl Azides. Inorg Chim Acta. 2014; 422:206–208.
174. Trofimenko, S. Photochemical Method for the Preparation of Substituted Polyhedral Borane Anions. US Patent. 3373098. Mar 12, 1968

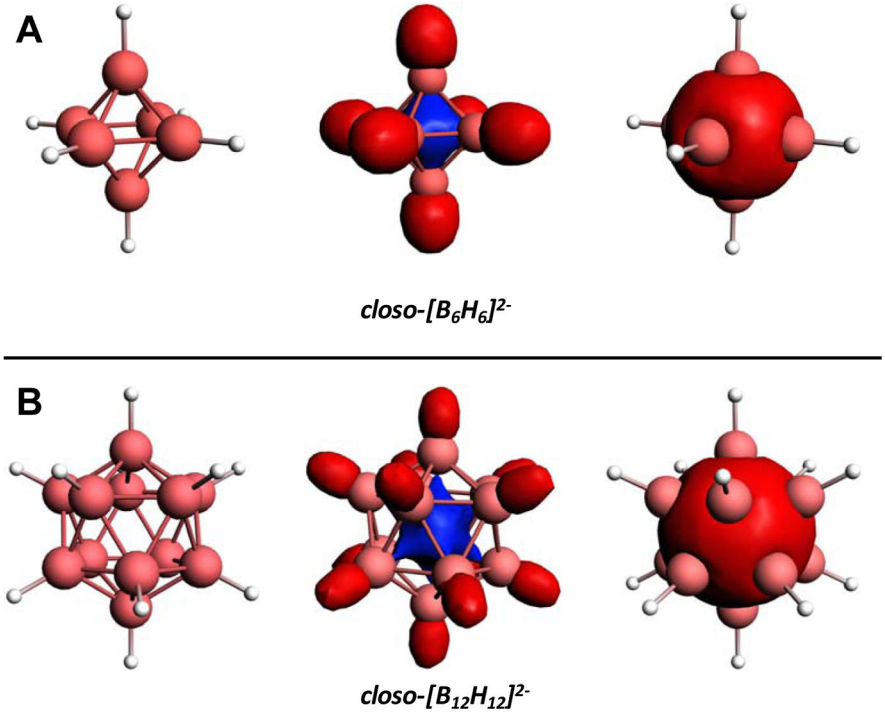

Figure 1.

Calculated structures (based on X-ray crystal structures) and representative Kohn-Sham molecular orbitals of A_{1g} symmetry demonstrating the delocalization of electron density in **A**. *closo*-$[B_6H_6]^{2-}$ and **B**. *closo*-$[B_{12}H_{12}]^{2-}$ as described by King.[21] This bonding arrangement gives rise to high kinetic stability relative to tri-coordinate and non-polyhedral boranes.

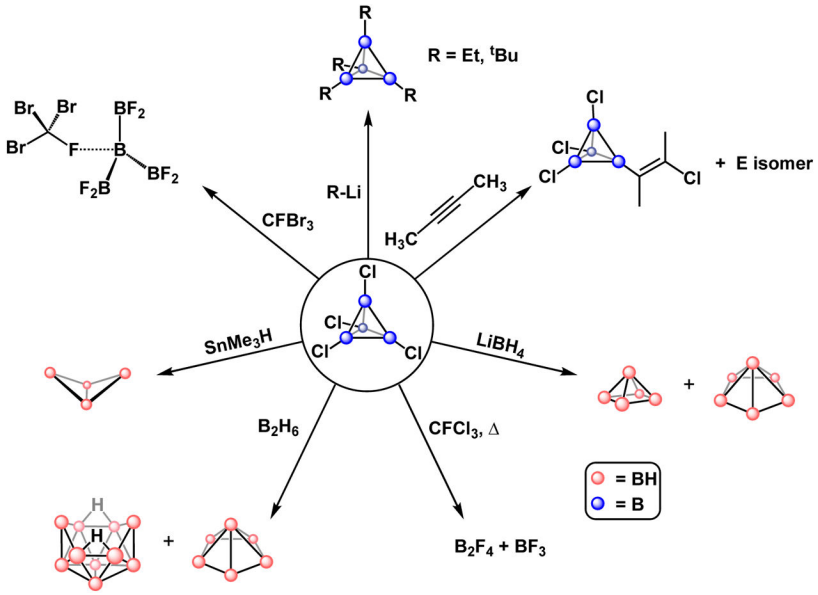

Figure 2.
Summary of reactivity of tetrachloro-*closo*-tetraborate.

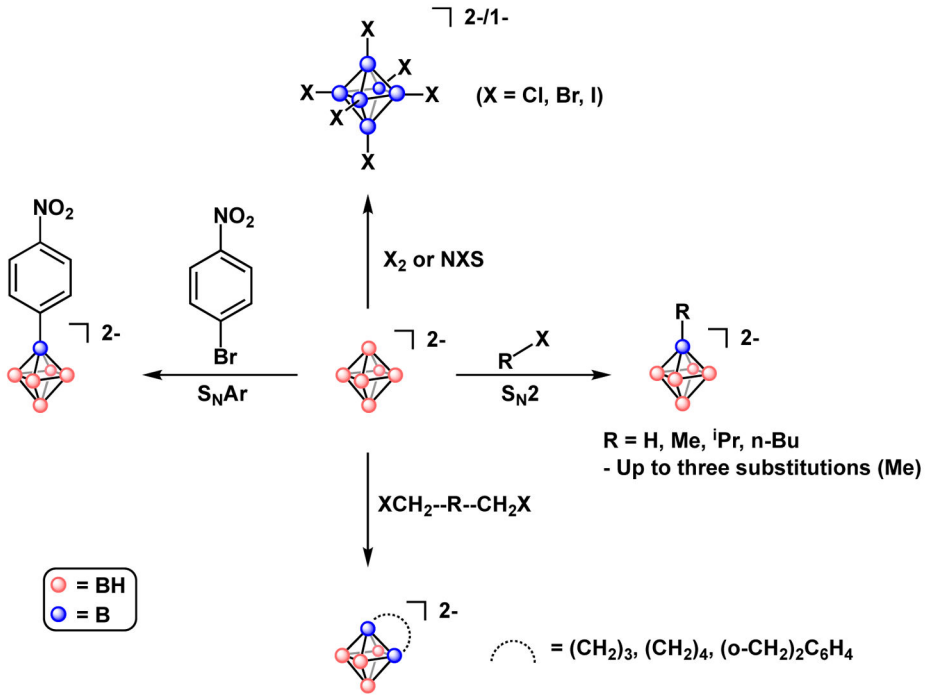

Figure 3.
Reactivity of *closo*-$[B_6H_6]^{2-}$, as described in the literature.

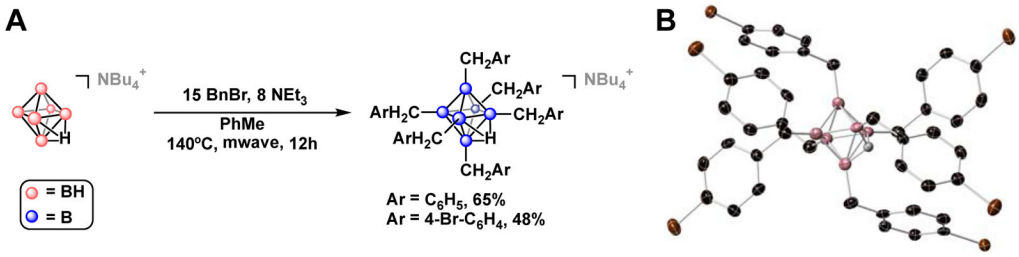

Figure 4.

A. Synthesis of perfunctionalized B_6 clusters featuring direct B–C bonds. **B.** X-ray crystal structure of *closo*-$[B_6(CH_2\text{-}4\text{-}Br\text{-}C_6H_4)_6H^{fac}]^{1-}$.

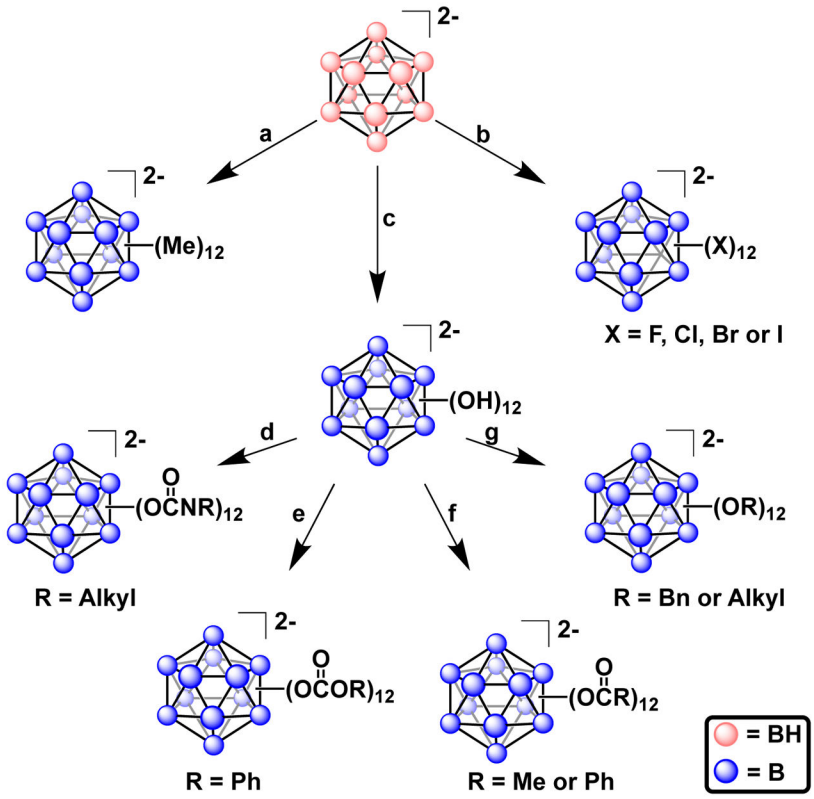

Figure 5.

Homoperfunctionalization of *closo*-$[B_{12}H_{12}]^{2-}$. Cations omitted for clarity. **a.** *Alkylation*. Peralkylation of dodecaborate can be achieved by refluxing $[N^nBu_4]_2[B_{12}H_{12}]$ with neat $AlMe_3$ and iodomethane over eleven days to form $[N^nBu_4]_2[B_{12}Me_{12}]$.[80] This remains the only reported peralkylation of dodecaborate, and the only homopersubstituted dodecaborate that contains B–C linkages. b) Halogenation[52,65–68] c) Hydroxylation[69–71,81] d) Carbamation[82] e) Carbonation[82] f) Esterification[72] g) Etherification[71].

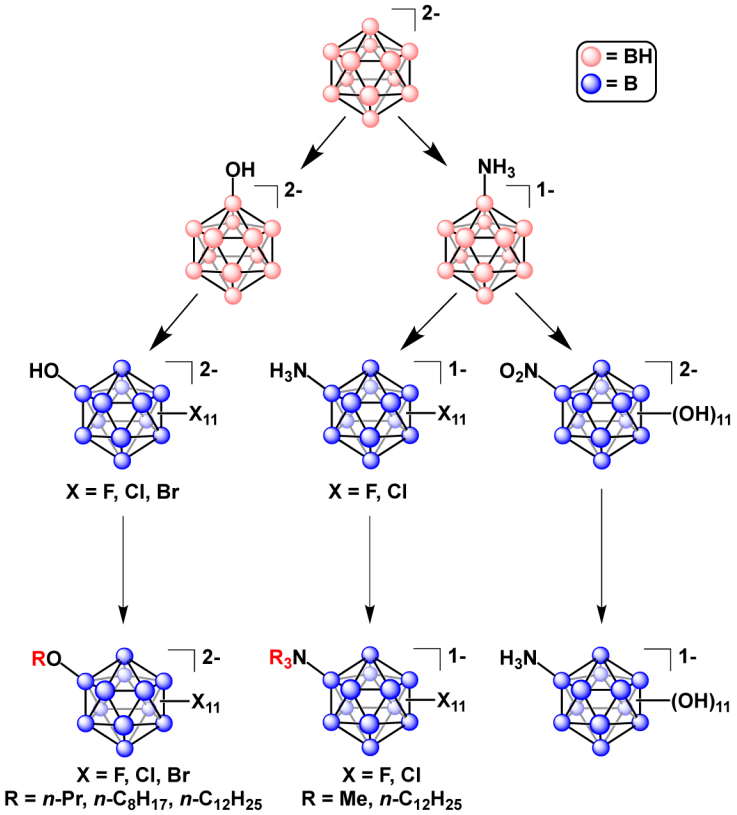

Figure 6.

Established routes for the heteroperfunctionalization of *closo*-$[B_{12}H_{12}]^{2-}$. Cations have been omitted for clarity.

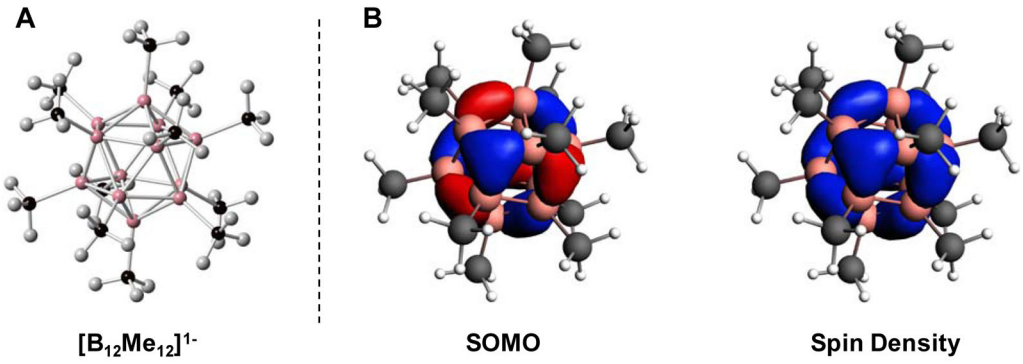

Figure 7.

A. X-ray crystal structure of $[(PPh_3)_2N][B_{12}Me_{12}]$ ($[(PPh_3)_2N]^+$ counterion omitted for clarity). **B.** The singly occupied molecular orbital (SOMO) and the spin density localization (PBE/D3BJ:TZP).

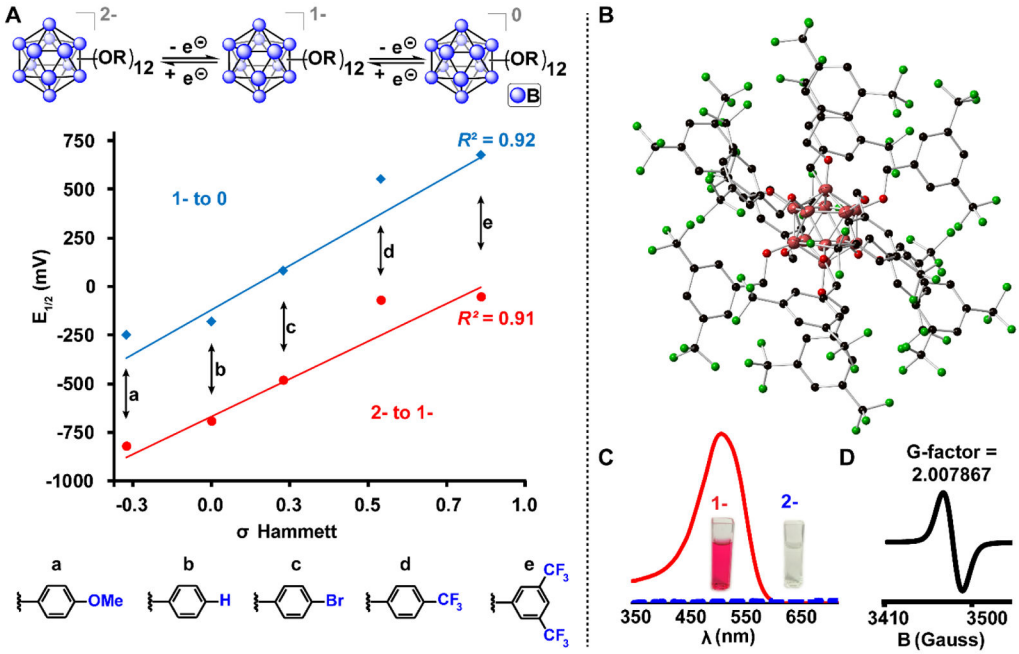

Figure 8.

A. Redox potentials of $[B_{12}(OR)_{12}]$ clusters plotted vs Hammett constants (top/blue = 1- to 0, bottom/red = 2- to 1-). **B**. Single crystal X-ray structure of cluster [**e**]$^{1-}$. **C**. UV-vis spectra and photos of the air-stable radical cluster [**e**]$^{1-}$ (red line) and the dianionic cluster [**e**]$^{2-}$ (blue dashed line). **D**. EPR spectrum of the radical cluster [**e**]$^{1-}$. These highlight the tunable nature of the perfunctionalized clusters.[10,44,95]

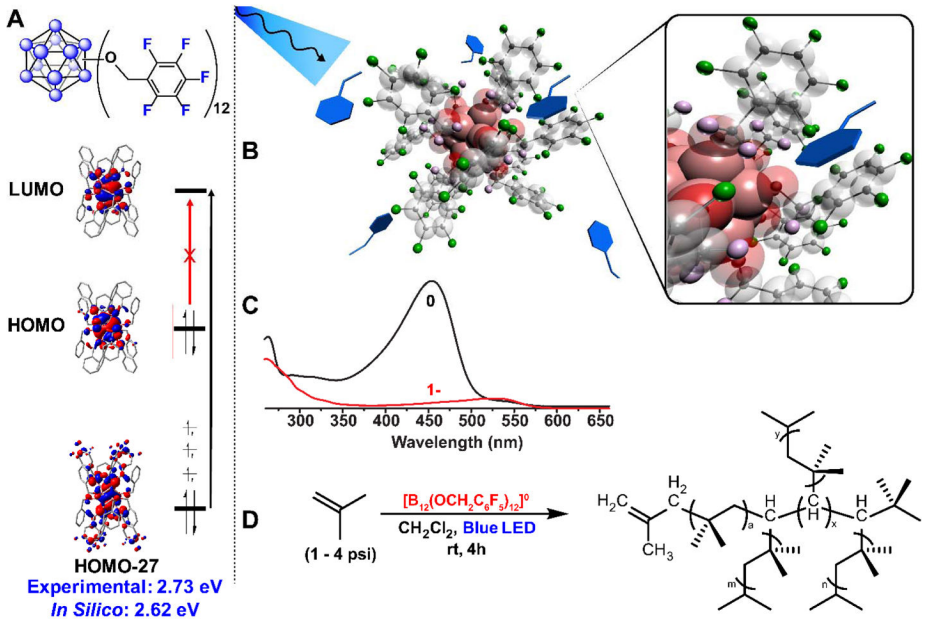

Figure 9.

A. TD-DFT calculation describing the charge-transfer excitation pathway in *hypercloso*-$B_{12}(OCH_2C_6F_5)_{12}$. **B**. Schematic representation of hypothesized docking of styrene monomers among the pentafluoroaryl groups of *hypercloso*-$B_{12}(OCH_2C_6F_5)_{12}$ which helps facilitate electron transfer. **C**. UV-vis absorption spectra for neutral *hypercloso*-$B_{12}(OCH_2C_6F_5)_{12}$ (black) and radical *hypocloso*-$[B_{12}(OCH_2C_6F_5)_{12}]^{1-}$ (red). **D**. Production of branched poly(isobutylene) initiated by $B_{12}(OCH_2C_6F_5)_{12}$ in the presence of blue LED light.

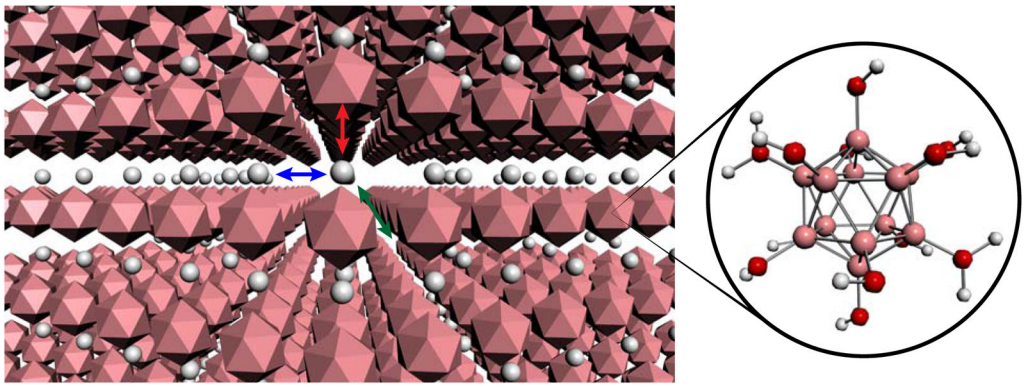

Figure 10.

Schematic representation of the crystal lattice of *closo*-$H_2[B_{12}(OH)_{12}]$ synthesized by Stasko and co-workers which was shown to conduct protons in the solid state.

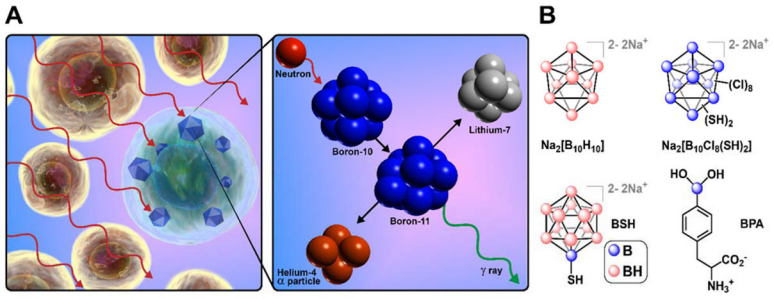

Figure 11.

A. An illustration of BNCT, a binary strategy for the treatment of cancer. **B**. Some BNCT candidates used in the preclinical and clinical settings.

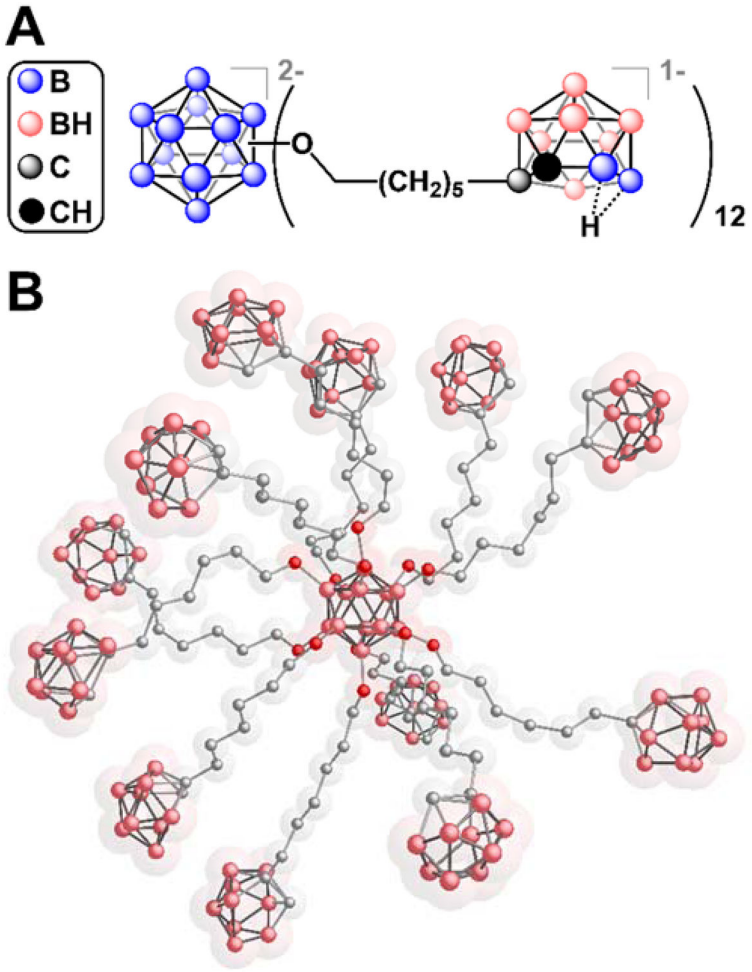

Figure 12.

A. The chemical structure and **B**. A 3D representation of the dodeca(*nido-o*-carboranyl)-substituted dodecaborate cluster.

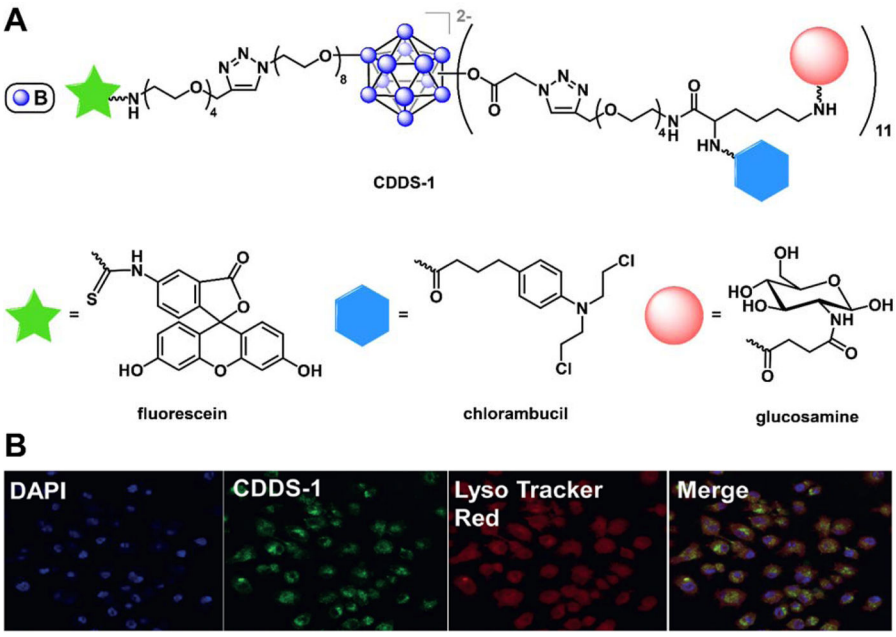

Figure 13.

A. A trimodal closomer drug delivery system, CDDS-**1**, features targeting, imaging, and cell-killing abilities. **B**. Confocal microscopy images of CDDS-**1** show its co-localization with lysosomes. Reprinted (adapted) with permission from Sarma, S. J.; Khan, A. A.; Goswami, L. N.; Jalisatgi, S. S.; Hawthorne, M. F. *Chem. Eur. J.* **2016**, *22*, 12715. Copyright 2016 Wiley-VCH Verlag GmbH & Co. KGaA, Weinheim.

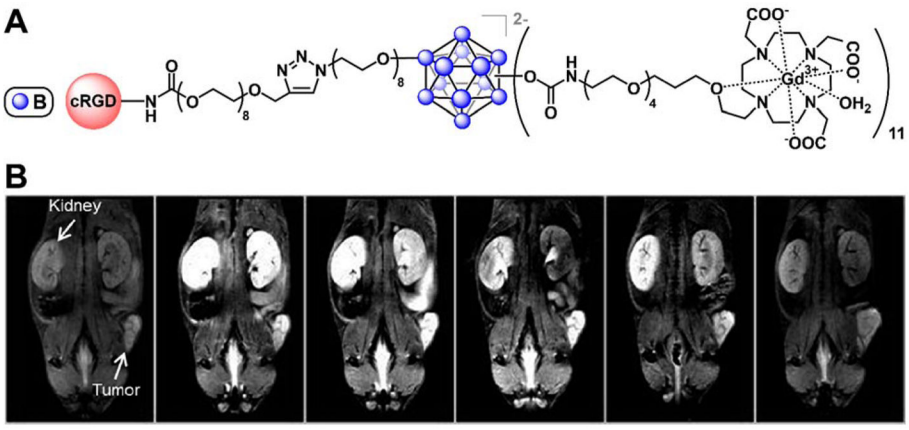

Figure 14.

A. The cRGD peptide-labeled, Gd^{3+}-DOTA chelates-carrying dodecaborate cluster MRI contrast agent and **B**. the resulting strong contrast enhancement in T1-weighted MRI scans of mice for up to 4 hours after injection. Reprinted (adapted) with permission from Goswami, L. N.; Ma, L.; Cai, Q.; Sarma, S. J.; Jalisatgi, S. S.; Hawthorne, M. F. *Inorg. Chem.* **2013**, *52*, 1701. Copyright 2013 American Chemical Society.

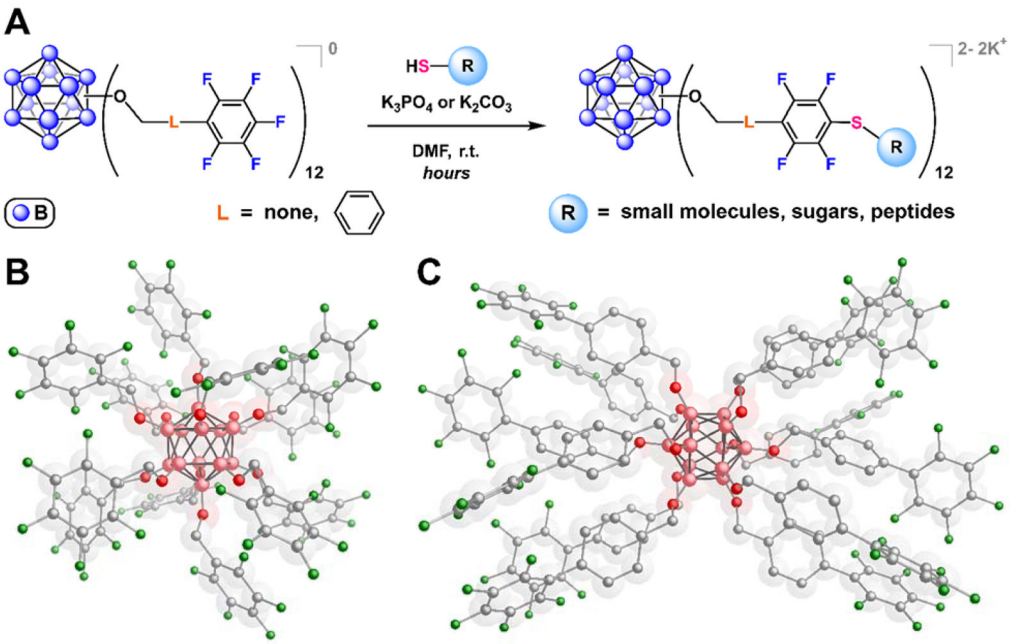

Figure 15.

A. The pentafluoroaryl-based dodecaborate clusters can undergo efficient S_NAr reactions with a variety of thiolated molecules. **B–C**. Single X-ray crystal structures of *hypercloso*-$B_{12}(OCH_2C_6F_5)_{12}$ (**B**) and *hypercloso*-$B_{12}(OCH_2\text{-}4\text{-}(C_6F_5)\text{-}C_6H_4)_{12}$ (**C**).

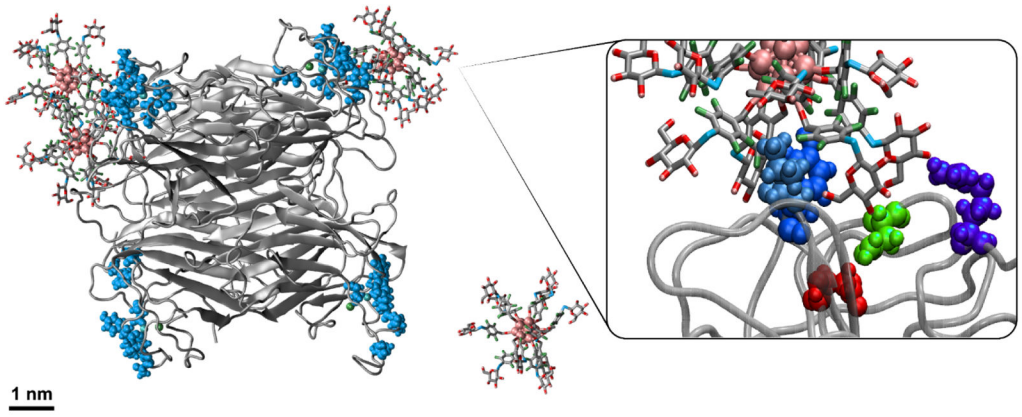

Figure 16.

A snapshot after 20 ns of a molecular dynamics simulation between a glycosylated OCN and the tetrameric lectin ConA. The carbohydrate-binding sites of ConA are highlighted.